School of Engineering and Information Technology

Intelligent Power Systems

Control and Management of a Microgrid
and the use of Droop Control

Authored by: Travis Wilson

Academic Supervisor: Dr. Greg Crebbin

A thesis submitted in partial fulfillment of the requirements for the degree of Bachelor of Engineering (Honours).

June 2015

Disclaimer

I declare that this thesis is my own account of my research and contains as its main content work, which has not previously been submitted for a degree at any tertiary education institution.

……..
Travis Wilson

Acknowledgements

I would first like to thank my supervisor, Dr. Greg Crebbin for not only providing initial guidance on the topic, but also for being there to answer any queries raised throughout the implementation of the project.

Secondly, I would like to thank the staff and students in the Energy and Engineering Faculty who have always been there to support questions not necessarily related to the topic in question but have accommodated random queries without fault.

Lastly, I would like to thank my family, especially my wife Rebekah who has been there to support me throughout this project and the rest of the program. Without her support this report would not have eventuate.

Abstract

Microgrids are a group of distributed generation systems that enable the support of local loads and have the ability to connect and disconnect to the main electrical utility grid. To respond to the increase in electrical power requirements from the customer base, Microgrids are a useful method of achieving network expansion, but have a number of protection issues related to reliability of supply, which is why the need of some form of microgrid control is required. This thesis report includes an analysis of droop control methods for control of a microgrid when connected to the distributed network, and when operating in islanded mode. The microgrid control strategies investigated as part of this report included an initial analysis of the various methods, and a more detailed analysis of synchronous generator control, including cooperative droop. This method has an improved response in regards to voltage regulation, frequency regulations and active power sharing. The use of droop control including primary and secondary control, to ensure the reliability of the network supply in the event of minor disruption includes events such as a load increase or decrease and larger disruptions that occur such as the loss of a generator, or the main electricity grid. It was found through the investigation of the governor control and the use of power-frequency droop control, that active power and frequency remained within the defined parameters of as set by the standard. Voltage regulation did have some events that caused the Distributed Generation (DG) voltage to exceed the limits, which is attributed to the grid-restoration event and would benefit from further investigation into control methods that would better support these types of events.

Table of Contents

List of Figures

List of Tables

Glossary

AFE	Active Front-End
AVR	Automatic Voltage Regulator
DG	Distributed Generation
DPC	Direct Power Control
LV	Low Voltage
MGCC	Micro-Grid Central Controller
MGCS	Micro-Grid Control Switch
MMO	Multi-Master Operation
MV	Medium Voltage
PCC	Point of Common Coupling
PLL	Phase-Locked Loop
PWM	Pulse Width Modulation
RMS	Root Mean Square
SG	Synchronous Generator
SMO	Single-Master Operation
ST	Switching Table
SWIN	South-West Interconnected Network
VSC	Voltage Source Converter
VSI	Voltage Source Inverter

Chapter 1

1 Introduction

1.1 Background

The introduction of renewable energy systems embedded in power distribution networks has become prevalent in the modern electrical power network. The use of loads and energy storage systems as controllable entities [1] [2] allows for Microgrid operation in both grid-connected and autonomous ('islanded') modes.

'Islanding' is when there is a electrical separation so that the network becomes two (or more) power systems, with each system operating independently of each other. These systems then operate independently and can support the local load requirements. This may occur when a fault occurs in the network and a section of the network is disconnected to protect equipment, the load or clear a fault.

When the island needs to reconnect to the main grid, synchronising relays are used when both the Microgrid and the distribution network have synchronised. Prior to this occurring it is necessary for the control and management of the Microgrid to ensure frequency, voltage, and angle are within the required limits to allow synchronisation.

This thesis project will investigate the control and management of a Microgrid when changing from islanded to grid-connected mode, concentrating on droop control methods and comparing to other forms of control to deal with the variety of renewable energy sources. These controllers are used to balance instantaneous variations in active and reactive demand on the network. For example frequency droop mode control can be used where there are multiple generators that share the responsibility of generator/load balance. By operating in droop mode the controller looks at the frequency of the power system and adjusts generator output from its nominal set point.

1.2 Objective

The aim of his thesis research project is to study the strategies for the control and management of micro-grids when operating in 'islanded' mode and when they are connected with the main power distribution network. The focus is on droop control and power management strategies for both converter and synchronous-machine-based units in Microgrids, as described in [1]. The approach taken in the development of the thesis is that of modelling the different types of controllers within PowerFactory™ associated with synchronous generator (SG) and Voltage Source Inverter (VSI), to determine performance characteristics in support of the literature review conducted within chapters 2 and 3.

1.3 Report Outline

Chapter 1 (this chapter) includes the introduction to the thesis topic, which covers the background information, objective and outline of the report.

Chapter 2 presents information about the Microgrid and the Distributed Network, the modes of operation, and also covers the reason behind the need for Microgrid controllers.

Chapter 3 covers different control strategies available, including different methods of droop control that can be used in the operation and management of a microgrid.

Chapter 4 outlines the investigation, and the specific models used in DIgSILENT PowerFactory™ to support the simulations in Chapter 5. This chapter also includes the scenarios investigated and discusses the possible use of MatLab Simulink to build controller models for import in PowerFactory™.

Chapter 5 captures the simulations conducted for the scenarios defined in Chapter 4 to determine the performance of the microgrid controller when exposed to various network events. It also provides the analysis of the results obtained from the simulations and discusses further scenarios that could be conducted that are not within the scope of this report.

Chapter 6 summarises the main outcomes of the thesis report and provides recommendations for further work that could be conducted, including future research topics, and projects to support further education.

Chapter 2

2 Microgrids and the Distributed Network

Microgrids

A Microgrid is a group of Distributed Generation (DG) units and loads connected together with a distribution system that can operate in three different modes of operation: islanded mode, grid-connected mode, and the transition between the two [3].

The use of Microgrids is a practical way of achieving a higher utilisation of renewable resources, the reduction of transmission losses, the lower capital investment for infrastructure, and the achievement of a more reliable electricity supply [4]. The major advantages being i) the provision of power during an emergency, or power shortage, ii) the use of plug-n-play technology, iii) the provision of power and frequency during islanded mode, and subsequent re-connection to the grid; and iv) the ability to share loads between the DGs when in islanded mode [5].

The local distributed network consists of a number of main components that create the Microgrid. These include the Distributed Generator (DG), the transmission system, the interconnection switch (also known as the Point of Common Coupling (PCC)), the control system, and various loads. This is then able to be connected to the main electricity grid through the PCC.

An example of a possible configuration of a Microgrid connected to the main grid is shown in Figure 1. This shows the interconnection between PV arrays, wind turbines, fuel cells, battery storage devices, other generation systems (like a diesel generator), and the loads that they support. In the event of a disconnection from the main electricity grid by the Microgrid Control Switch (MGCS) at the Point of Common Coupling (PCC), the Distributed Generation (DG) system will support the local load power requirements.

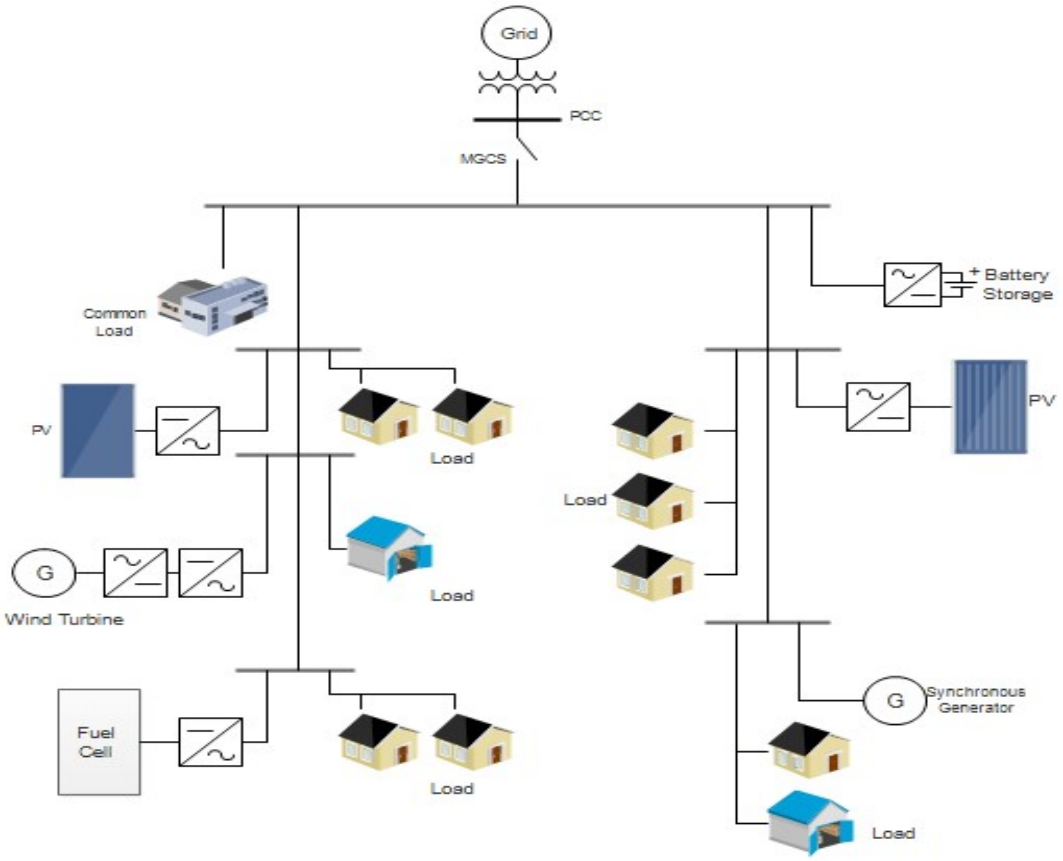

Figure 1: Possible MV Microgrid Network

2.1 Microgrid Operation

There are three modes of operation for the Microgrid namely grid-connected, islanded and transitions between the two modes [6]. Below is a description of these modes and the impact to the operation of the Microgrids, including the various issues with each.

2.1.1 Grid-connected Mode

This mode is when the Microgrid is connected to the main electricity supply grid and is the normal mode of operation. In this configuration the loads throughout the distribution network are supplied by the grid and DG units depending on load demand. The regulation of the voltage and frequency of the network is controlled by the utility grid [7]. In most cases the DG units may or may not provide power sharing with the network.

2.1.2 Islanded Mode

When the Microgrid is in islanded mode, through the loss of the grid supply, fluctuations in the frequency or power from the microgrid, or any other reason

such as maintenance, the microgrid will operate autonomously [8]. Through this autonomous operation the voltage and frequency of the Microgrid will be controlled by the DG units where they are required to provide the regulation and stable supply to the loads, and the real and reactive power is shared [9]. There are different methods used to enact this control, which are described in chapter 3 of this report, that enable the DG units to minimize the voltage and frequency variation between what is supplied and what is the nominal value.

The main limitations associated with a Microgrid operating in islanded mode include the need for load shedding [10], if voltage or frequency cannot be maintained at nominal levels, power quality requiring sufficient reactive power supply, and the delay in the response time of some generator units. These are among some of the issues when operating in this mode and are explained further in chapter 3.

2.1.3 Transition between Grid-connected and Islanding Mode

The time taken for the Microgrid to transition between grid-connected and islanded mode, and vice-versa needs to be minimized to ensure supply stability. This is where the interconnecting switch, such as the MGCS, which includes a controller, adjusts the power reference to match the nominal value [8].

For the limitation associated with active power and frequency when re-connecting to the main electricity grid, there are different values depending on whether the generating unit is dispatchable. For the South West Interconnected Network (SWIN) located in Western Australia these can be found in [11]. This indicates a Microgrid network operating at 6kV and above is required to maintain 90% of the nominal voltage and have a maximum steady-state voltage of 110% of nominal voltage [9]. For network operating below 6kV, this is reduced to +/-6% of nominal value during normal operating state, which is what the simulations in chapter 5 will address. These values differ for the switching times, during transients, which is discussed further in the simulation network analysis in chapter 5.

2.2 Microgrid Problems with Operation

The reason behind the regulation of Microgrids and their connection to the main electricity grid through a MGCS is due to the problems associated with Microgrids. The main technical challenges associated with Microgrid operation are the i) voltage and frequency control, ii) islanding, and iii) the protection of Microgrids [5].

2.2.1 Voltage and Frequency Control

When connected to the main electricity grid the active and reactive power that is generated is balanced with the consumed power by the loads of both Microgrid and main electricity grid, including any line losses [5]. When the Microgrid is disconnected and in islanded mode, the active and reactive power needs to be controlled by the microsources forming the DG units. This is conducted through voltage and frequency control of one or more of the microsources [8] which regulate the power sharing within the Microgrid, to avoid circulating current among DG units [1]. Alternatively, load shedding may occur if the frequency cannot be maintained within set limits to restore the Microgrid supply to the defined parameter limits.

2.2.2 Islanding

In islanding mode, which is the separation of the Microgrid from the main electrical supply, the Microgrid control strategies are important to ensure stable supply of electricity to the loads. Additionally when the Microgrid re-connects to the main grid, the voltage and frequency needs to be within acceptable limits otherwise it will not be connected through the MGCS, as managed by the MGCC. The control strategies adopted to maintain suitable parameters for the Microgrid are predominately droop controllers due to not requiring a communication system and avoidance of single points of failure for the stable and reliable operation of the system [12]. The droop control and other methods of control are explained further in chapter 3; which also defines the hierarchical control levels.

2.2.3 Protection

The most important issue that has arisen regarding Microgrids and their implementation is the protection system. This includes assuring the load,

distribution lines and the DGs are protected [5]. A protection scheme may consist of overcurrent synchronous based DGs [13], and directional overcurrent relays to protect the distribution lines [5] [13] during both islanded and grid-connected modes. Different protection schemes are used with a common form being the coordination of the directional overcurrent relays [5]. This topic is beyond the scope of the thesis topic and is discussion at length in [13] and [14].

Chapter 3

3 Microgrid Control

There are three levels of control undertaken for a Microgrid when interfaced to the main utility grid. These levels are explained further throughout this report under the individual methods of control but are summarised below, including the level of control and how they are applied.

3.1 Hierarchical Control Levels of a Microgrid

The main levels of control of a Microgrid are shown in Figure 2, and discussed further below.

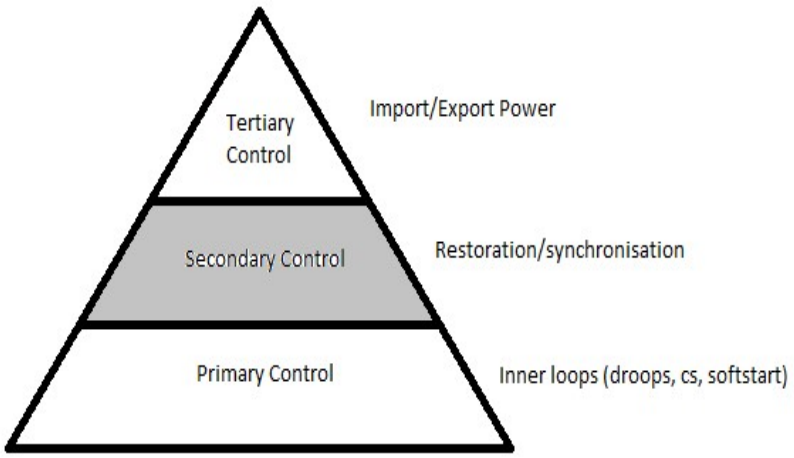

Figure 2: Microgrid (MG) Hierarchical control levels [15]

For primary (level 0 and level 1) MG control, the concept is the control of the DG microsource through a decentralised control system, such as droop control method, which is further explained in section 3.3. This form of control is used to dampen the system to increase stability [15]. Level 0 control includes current and voltage feedback and feedforward integration to regulate the module.

The secondary (level 2) control method includes a synchronization control loop to enable the disconnection and re-connection to the main grid to occur without disturbance to the supply power and frequency. This method ensures the DG microsource electrical levels are within the required levels.

Tertiary (level 3) control is concerned with the energy production level [15] controls of the power between the main grid and the Microgrid, or DG microsources within the Microgrid.

Additionally, there is another level of control (level 0), but this relates to the inner control loops that regulate output voltage and current to maintain system stability.

The method of how these levels of control interact with each other is represented further in Figure 3, which shows an example of interaction of the control methods for a frequency deviation in the Microgrid.

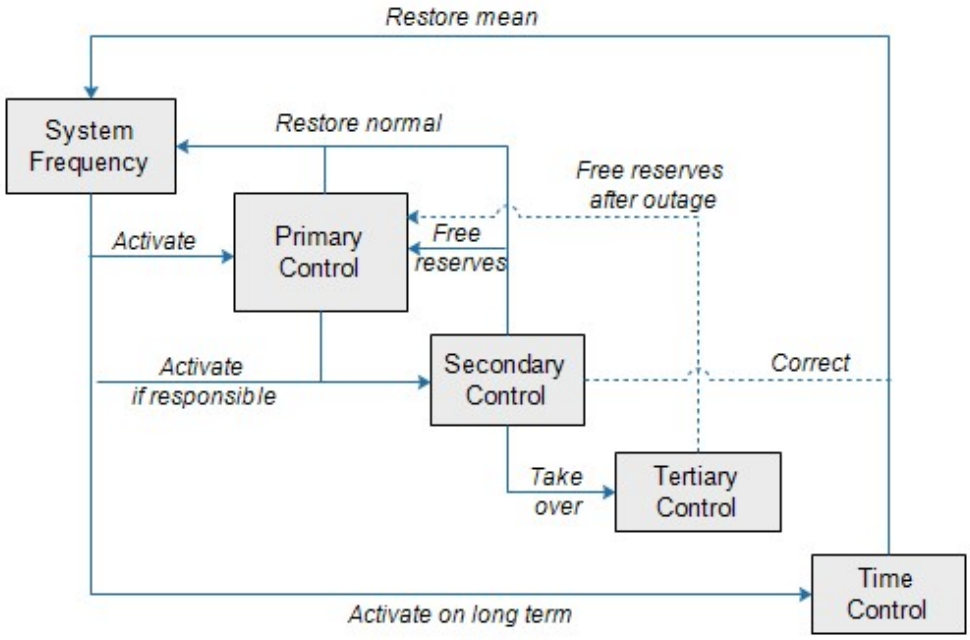

Figure 3: Frame for multilevel control [15].

3.2 Common Methods of Control

A Microgrid that is connected to the main utility grid may experience an event that is not planned (eg. fault event), or planned (eg. maintenance) where the main grid source is lost. In this situation the local generation profile of the Microgrid may need to be modified to accommodate the load imbalance by varying the load distributed between generation units. This allows for the disconnection transient to be reduced.

To ensure the generation-load balance is maintained and disconnection transient is reduced, means of control are used, including the use of a Voltage Source Inverter (VSI), as shown in Figure 4, or via Synchronous Generator (SG) control means. There are many means in which a Microgrid can be controlled, with common control means including those detailed below.

Figure 4 shows a single-phase version of control where the voltage and current are used to calculate the active (P) and reactive (Q) powers. The output voltages are then used as reference signals for the VSI switching sequence, using PWN modulation [16].

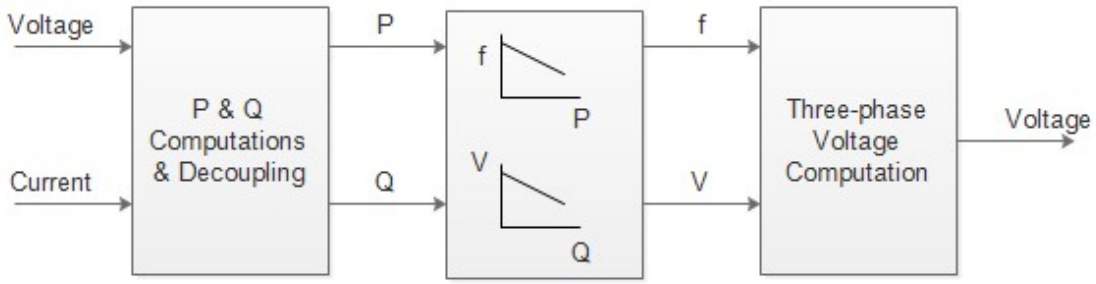

Figure 4: Simplified VSI Model [16].

3.2.1 Single-Master Operation

One method of control of a micro-grid involves the Single-Master Operation (SMO) method of operation. This is where a voltage source inverter (VSI) acts as the master, in islanded mode, and establishes the voltage reference when the main power source is disconnected or lost. The other inverters then act in PQ (slave) mode.

For this operation the local DG microsources are able to receive the required information from the Micro-Grid Central Controller (MGCC) including the generation profile and subsequently control dependent on the corresponding micro-source. An example of this type of control is shown in Figure 5 [16].

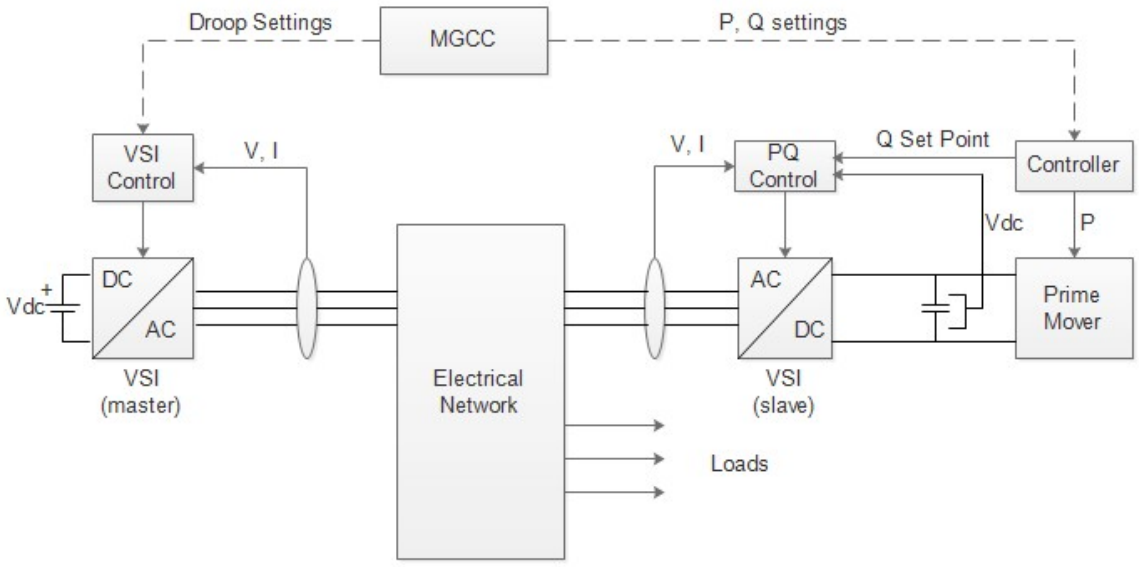

Figure 5: Single-Master Control during islanded operation [16].

The main limitations associated with this type of control include the need to locate a secondary load-frequency control as described in 3.2.3. This is required during islanded operation, and needs to be installed in a micro-source that can be controlled.

3.2.2 Multi-Master Operation

An adaptation of the SMO method is to include a secondary master source. This is where several inverters are operating as VSI with pre-defined frequency/active power and voltage/reactive power characteristics. This is decentralised control and removes the requirement for communications network which can be costly, and has allowance for plug-n-play capabilities for the loads and DG units [17].

An example of this type of controller is shown in Figure 6 [16].

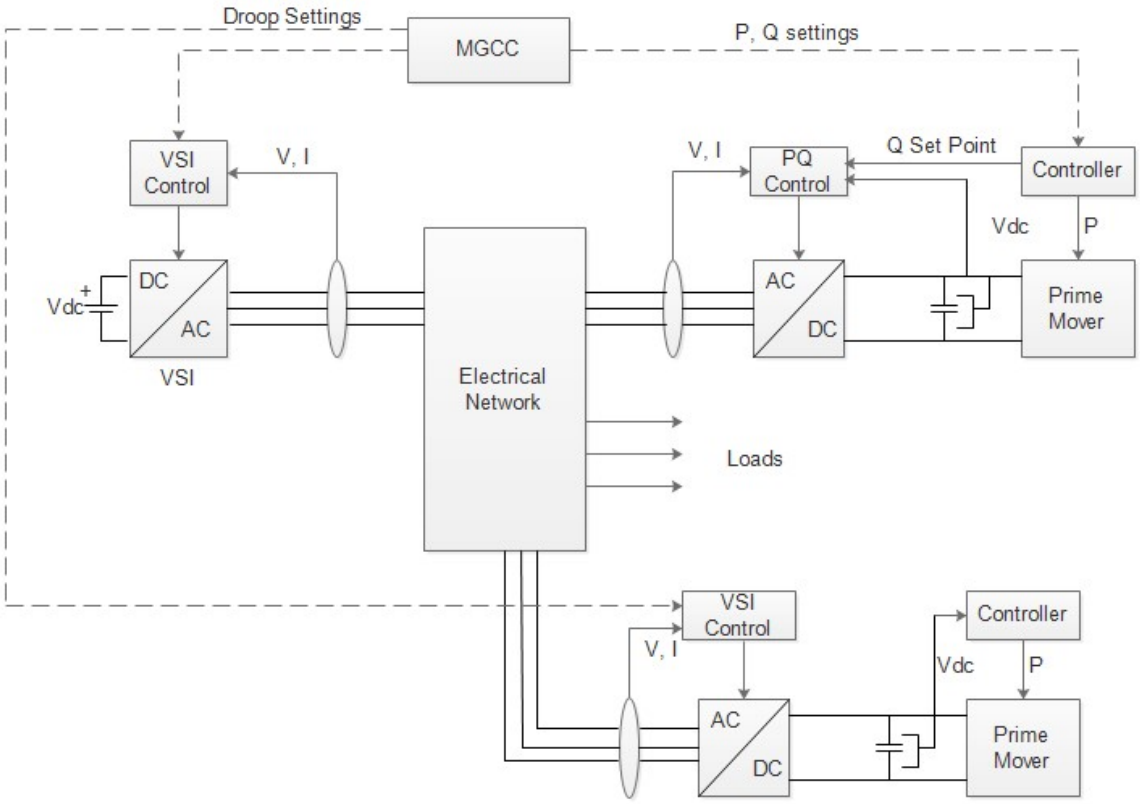

Figure 6: Multi-Master Control during islanded operation [16].

As per the SMO method of control, the MMO control requires a secondary load-frequency controller during islanded operation.

3.2.3 Secondary Load-Frequency Control

Another method of Microgrid control is by using a secondary load-frequency. This method involves the use of storage devices, such as batteries, to inject or absorb active power to maintain frequency stability. As the storage units are only responsible for load-frequency control during the transient period, this method should only be applied then due to the limited storage capacity.

The benefit of this method of control is to correct frequency deviations during conditions of islanded operation as the storage devices would continually inject power even if the frequency stablises at a level other than the desired. Equation (1) shows how the VSI active power output as shown in Figure 4 is proportional to the Microgrid frequency deviation [16].

$$\Delta\omega = \omega_{0i} - k_{Pi}P_i - [\omega_{0i} - k_{Pi}(P_i + \Delta P_i)] = k_{Pi}\Delta P_i \quad (1)$$

Where $\omega_0 = angular\ frequency\ of\ the\ inverter$

$k_P = droop\ slope\ of\ inverter$

$P = inverter\ active\ power$

$Note: i\ denotes\ initial\ value$

An example of a local secondary load-frequency control for microsources that can be controlled is shown in Figure 7 [16]. This shows the introduction of a proportional/integral (PI) controller at each controllable microsource. Another option is to use a Microgrid Centralised Controller (MGCC).

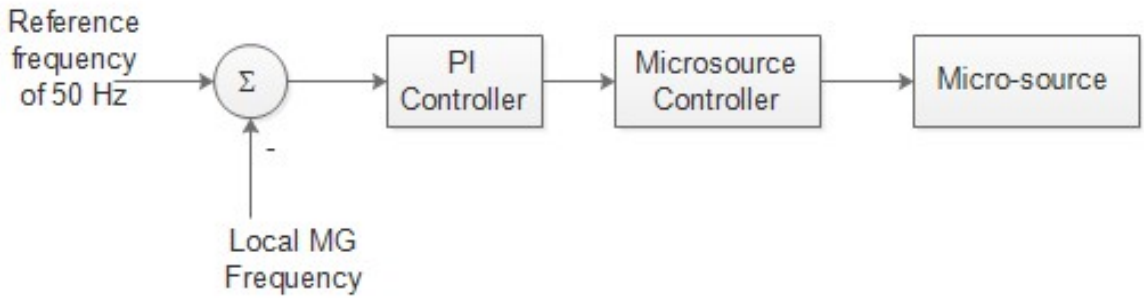

Figure 7: Secondary load-frequency controller [16].

This type of controller is limited to use during the transient stage as this is when the storage devices have responsibility for the load-frequency primary control.

3.2.4 Allocation of Fixed and Switching Capacitors

This method of Microgrid control involves the allocation of fixed and switching capacitors throughout the network. This supplies the Microgrid during both normal operating conditions and islanded mode to assist with maintaining the required reactive power. This is beneficial in that it helps the utility generators maintain maximum power generation, whereas without the switching capacitors the control of active and reactive power comes as a compromise to generating capacity [3].

To ensure optimum placement of the switching capacitors within the Microgrid, there is normally a need to model the system to ensure bus voltages within the Microgrid are maintained within the set limits in both islanded and grid-connected modes.

3.2.5 Direct Power Control (DPC)

The use of Direct Power Control (DPC) is more utilised than the other methods described above. This method uses three-phase, phase active rectifiers interfaced with regenerative loads connected to the grid. This method is based on the regulation of instantaneous real and reactive powers.

This method involves the use of a look-up table, otherwise known as a Switching Table (ST) [18]. The purpose of the ST is to accurately track the instantaneous power to enable regulation of the real and reactive powers, via switching state selection from the ST. Different STs can be used during the rectifier and inverter operation modes, minimizing switching losses thereby improving efficiency. This is more beneficial than the use of just one ST.

The use of the ST, as shown in Figure 8, highlights how the ST influences the active (P) and reactive (Q) powers using an active front-end (AFE) two-level voltage source converter (VSC).

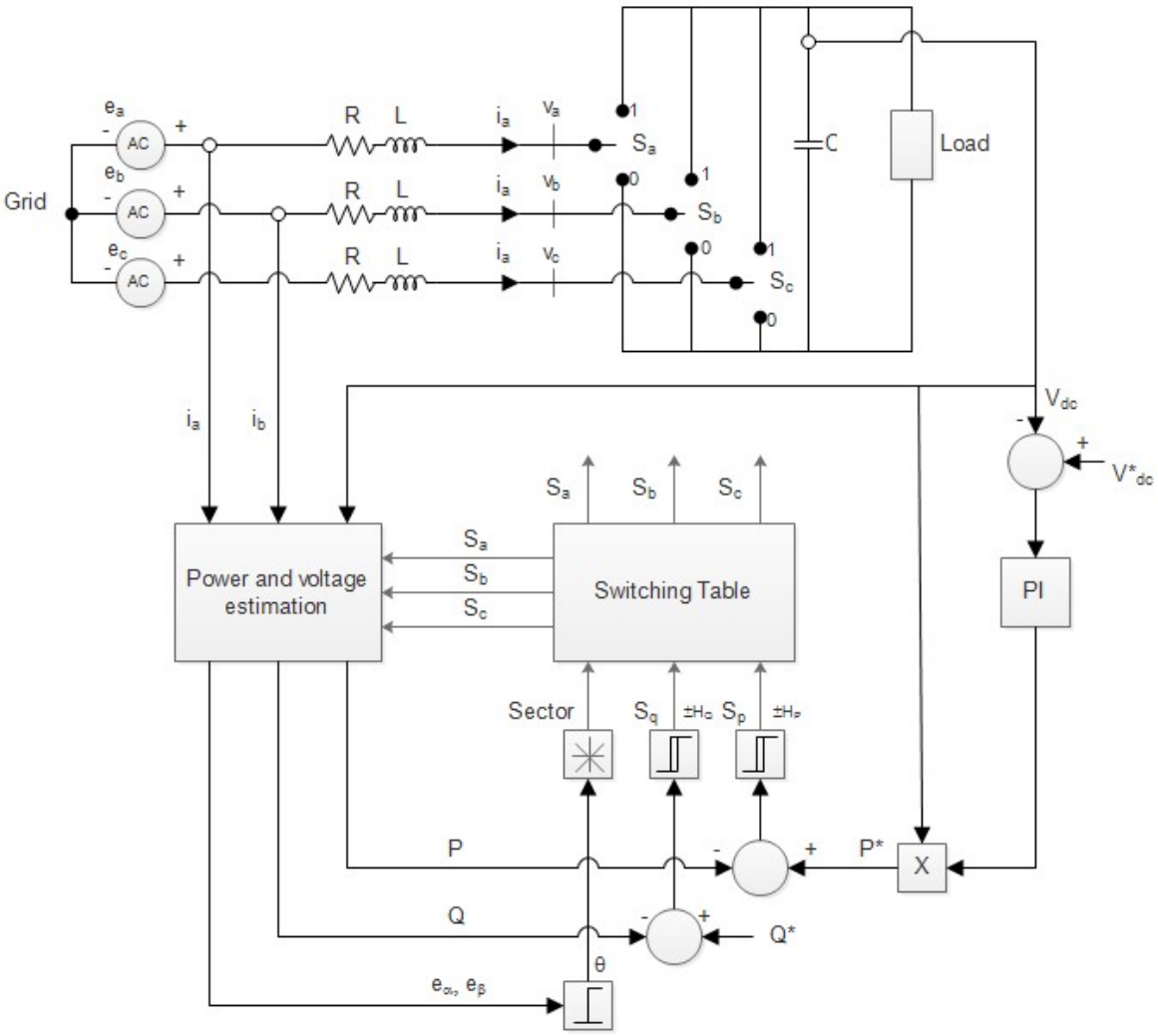

Figure 8: DPC Method [18].

Though this has been adopted as a common strategy for Microgrid control, it has relatively complex configuration due to the use of coordinate transformation blocks. Also the use of current regulation loops means the voltage-orientated control performance is dependent on the quality of the current control application strategy.

3.3 Droop Control

There are various forms of droop control utilised, with the main objective being the management of the real and reactive power demand within the Microgrid [1]. The principle behind this form of control consists of emulating virtual inertias (Synchronous Generators), or through Voltage-Source Converters (VSC) [9], by subtracting proportional parts of the average active and reactive powers from the frequency and amplitude of each other [15].

The SG form of Microgrid control involves the speed control mode of the prime mover (i.e. diesel generator in this case) driving a SG connected to the main electrical grid. It allows the SG to run in parallel, so that loads are shared among operators in proportion to their power ratings.

The active (P) and reactive (Q) powers produced by the generators are shown in equations (2) and (3) [1] where the active power (P) and reactive power (Q) values are affected by the voltage angle δ, or power angle, which is simplified when δ is set to zero.

$$P = \frac{E}{R^2 + X^2}(XVsin\delta + R(E - Vcos\delta)) \quad (2)$$

$$Q = \frac{E}{R^2 + X^2}(-RVsin\delta + X(E - Vcos\delta)) \quad (3)$$

Alternatively with the VSC-based interface, the usual method of interface to the main grid [19], where the active and reactive power sharing is conducted through control of the voltage and frequency (VSI Mode), or the active and reactive power (PQ mode) of the system through local feedback [19], depending on the inverter mode.

3.3.1 SG Droop Control

For primary control methods using the SG the prime mover has a droop governor, where the prime mover speed decreases upon the application of a greater load, causing a decrease in frequency. The rate of frequency decrease to the load increase forms the droop value, as shown in Figure 10. After the load increase has occurred, the resulting frequency after the droop stabilises close to the nominal value, with the frequency deviation being proportional to the load change and the droop value of the primary control [20], as shown in Figure 9. This method of control forms part of the analysis of this thesis and is shown further in chapters 4 and 5.

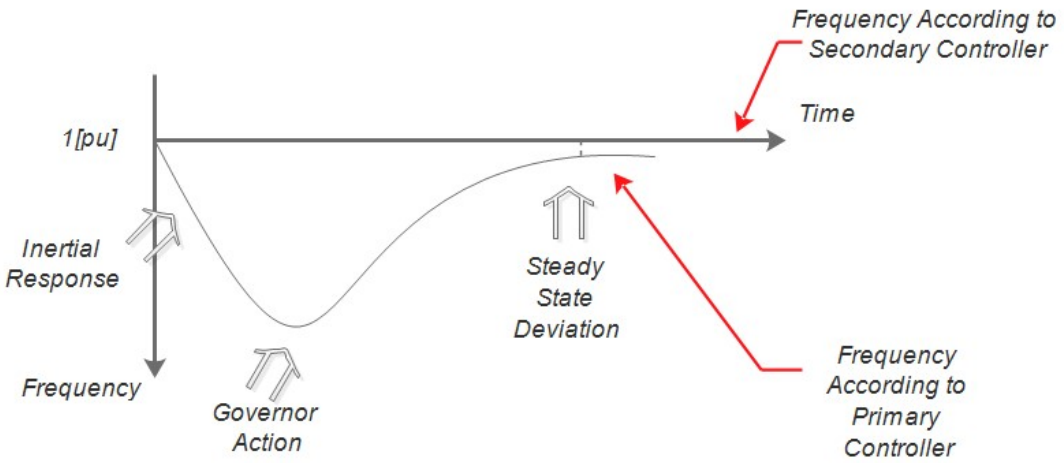

Figure 9: Frequency deviation after an increase in load [21].

This speed droop value of a governor is defined by equation (4) where η_{nl} and η_{fl} represent the no load and full load prime mover speeds, with most governors having a speed-droop value of between 2 and 4 percent [22]. In addition to this most governors have a set point adjustment which allows the no-load speed of the turbine to be adjusted.

$$Speed\ Droop = \frac{\eta_{nl} - \eta_{fl}}{\eta_{fl}} \tag{4}$$

The resulting speed vs power, and frequency vs power curves shown in Figure 10 represent how the change in speed or frequency impacts the output power from the generator.

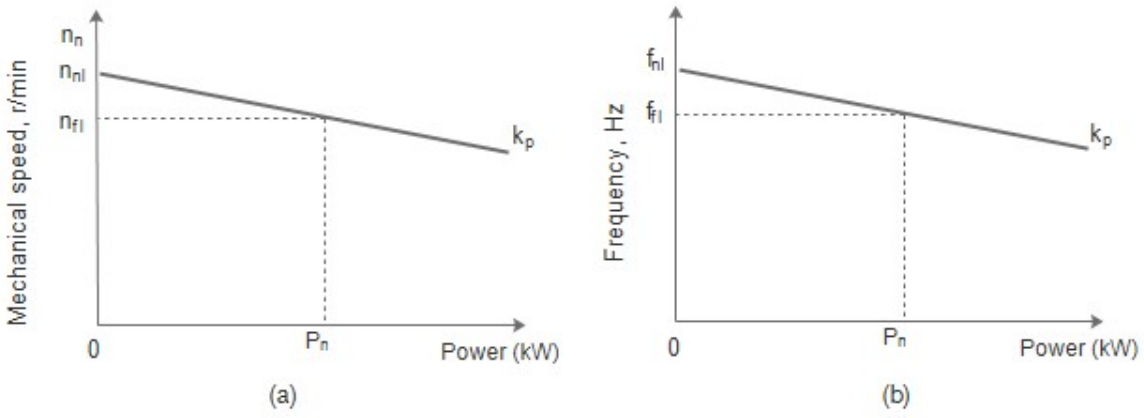

Figure 10: Ideal characteristics of a governor with speed droop [21].

Due to the frequency deviation caused by the load increase, to restore the frequency to the nominal value, a secondary supplementary controller is required. This controls the power source set points to adjust the power reference set points. Due to its slower reaction time this controller overrides the frequency deviation [20].

Further information is relation to the operation of the prime mover, synchronous generators and inertial response can be sourced from [21], and is not discussed further in this thesis.

3.3.2 VSC Droop Control

For VSC-based control there are various forms that are available which enable control of the DG units within the microgrid in islanded mode. This type of control uses inverters to interface with the grid. This is a common form used that allows for an easy plug and play technology, but requires some form of control to maintain stability. The two modes of this control used with inverters include the P-Q mode and VSI mode.

3.3.2.1 Active power-reactive power (P-Q) inverter control

The active power (P) and reactive power (Q) mode is the 'slave' mode as it does not control the frequency of the grid, only through the use of a Phase-Lock Loop (PLL) device does it follow the current grid frequency. The P-Q inverter provides a stable active and reactive power setpoint for support during grid-connected mode and supports grid power quality by injecting its input power.

Equation (5) shows how the power in relation to the frequency, P(f) is affected by the delivered power from the inverter (P_0) minus the rate of change of the droop (k_f) in MW/Hz in relation to the frequency setpoint (f_{set}).

$$P(f) = P_o - k_f(f_{set} - f) \tag{5}$$

In the event the reactive power and voltage (Q-V) droop is used the terminal voltage is measured for comparison to the referenced value, and the reactive power of the inverter is adjusted accordingly [23]. This is represented by

equation (6), where the reactive power in relation to the terminal voltage, Q(V) is determined by the values of consumed or delivered reactive power (Q_0), the voltage setpoint (V_{set}) and rate of change of the droop (k_v) in MVar/V.

$$Q(V) = Q_o - k_v(V_{set} - V) \quad (6)$$

This type of control is problematic in relation to the measurement of active power and is referred to as a V-f inverter.

3.3.2.2 *Voltage Source Inverter (VSI) control*

In contrast to the P-Q method, the droop control using a VSI measures the active and reactive powers from the terminal outputs. Here the active power (P) is used in reference to a setpoint P_{set} and rate of change of the droop, in ƒ/MW, to find the frequency variation, as shown in equation (7).

$$f(P) = k_p(P_{set} - P) - f_o \quad (7)$$

This is also the case for determining the change in reactive power in relation to the voltage, Q(V) as shown in equation (8), where the voltage setpoint V_{set} and rate of change of the droop value, in MVar/V, impacts the resulting reactive power value.

$$Q(V) = Q_o - k_v(V_{set} - V) \quad (8)$$

3.3.3 Voltage Droop Control

Voltage Droop Control is a conventional method that consists of adjusting the output voltage frequency and amplitude to achieve autonomous power sharing without control wire interconnections. This form of control is especially beneficial in the control of low voltage (LV) Microgrids with a high degree of renewable energy microsources [12].

This controller operates by using the terminal voltage to determine the priority of the power changes, so that renewable microsources changing the power they produce, does not impact the reliability of the Microgrid network. In an islanded situation, the use of at least one DG unit will have voltage-based droop control to set the reference voltage for the controllers to enable power sharing and balancing [12] [24]. The lack of any need to have some form of communications established for the voltage-based droop controller allows for easier implementation into renewable energy microsources where power sharing and voltage is controlled in islanded mode. Additionally, this controller does not require changing during grid-connected network operation.

3.3.4 Frequency Droop Control

Frequency Droop Control is adopted more than other methods and is where the controller uses real power output of the generator to calculate the ideal operating frequency. This allows the SG to dampen the fast effects of changing loads, increasing the stability of the system. This method has a proportional only controller for frequency and voltage, with no form of integral control [24] and tends to be implemented with some form of angle droop control to improve performance due to limitations associated with permanent frequency offset seen with most decentralised configurations as described in section 3.2.2.

The frequency droop controller has similar benefits to other droop controllers in that it does not need a communications system, where it is beneficial to measure voltage and frequency locally [25]. There is plenty of literature on the use of frequency only control available, and is only used as one component of the control method used in this thesis so will not be discussed any further.

3.3.5 Angle Droop Control and Power Sharing

This controller type is where the instantaneous real and reactive powers from the DG to the Microgrid are passed through a low pass filter to obtain average real (P) and reactive (Q) power to enables much lower frequency deviation as compared to conventional frequency droop control [9]. This is beneficial when the power sharing among parallel sources is required so the need to control the voltage magnitude and frequency is paramount.

Equations (9) and (10) [19] show the instantaneous real power (P) and reactive power (Q) from the DG unit with the angle difference within equation (10) being small enough to have very little impact therefore reactive power control is predominately controlled using the voltage. Also with the active power control, this can be managed through manipulation of the angle difference.

$$P = \frac{VV_t \sin(\delta - \delta_t)}{X_f} \tag{9}$$

$$Q = \frac{V^2 - VV_t \cos(\delta - \delta_t)}{X_f} \tag{10}$$

$P = instantaneous\ real\ power$

$Q = reactive\ power$

$V = voltage$

$V_t = Microgrid\ voltage\ at\ the\ bus$

$\delta = angle$

$\delta_t = angle\ at\ the\ bus$

$X_f = output\ impedance$

The angle droop controller, its performance in comparison with the frequency controller and its ability to power share with a much lower frequency deviation compared to frequency droop, enables better quality and system stability when there are frequent load changes within the microgrid network [9], [19].

3.3.6 Cooperative Droop Control

Cooperative droop control is where more than one form of control is used for the power management strategy for both converter-based and synchronous-machine-based units within the microgrid. An example of this form of droop control is the combination of angle and frequency droop control as described above in sections 3.3.4 and 3.3.5, and shown in [1] where the angle-frequency (δ-f) droop controller is investigated.

The benefit associated with the use of a cooperative droop controller, like the angle-frequency controller is better power sharing accuracy and more degrees of freedom given the availability of more droop parameters associated with the two control loops. This enables the improvement on static and dynamic performance when tuned correctly [1].

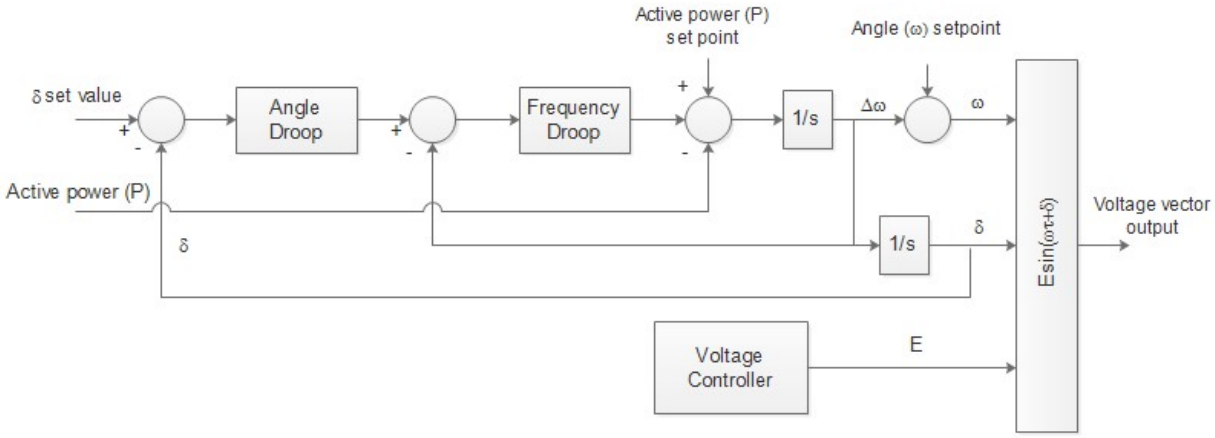

Figure 11: Angle-frequency droop controller [1].

The example controller shown in Figure 11, shows how the combination of angle-frequency droops with standard voltage droop control allows for damping of angle and frequency oscillations and synchronising power [1]. The components of the damping conducted by the frequency droop, and the synchronising by the angle droop are shown is equations (11) and (12) [1], where the frequency droop gain K_f and the change in angular frequency affect the damping power; similarly the frequency droop gain K_f, angle droop gain K_d and the change in the delta angle affects the synchronising power.

$$damping\ power = \Delta P_{damp} = -K_f \Delta\omega \quad (11)$$

$$synchronising\ power = \Delta P_{synch} = -K_f K_d \Delta\delta \quad (12)$$

This type of droop controller has much better control than that exhibited by the simpler frequency droop, or angle droop controllers described.

3.3.7 Virtual Flux Droop Method

Virtual Flux Droop Method is a new control strategy that acts by 'drooping' the virtual flux instead of the inverter output voltage. This is where the relationship between the inverter virtual flux and the active and reactive powers is defined to develop the flux droop method. Here, dropping the flux amplitude and controlling the phase angle achieve the power sharing. With this method multi-feedback loops and Pulse-Width Modulators (PWMs) are not needed.

The use of this form of droop control is relatively new and is discussed further in [26]. It is mentioned within this thesis paper due to being another form of droop control that could possibly be investigated further but is outside the scope of this thesis.

Chapter 4

4 Investigation

This chapter will form the basis of the thesis investigation on the performance of the synchronous generator governor and power-frequency droop controller through simulations run within the DIgSILENT PowerFactory™ simulation software and supported by simulations with MathWorks Simulink, including the Simscape and SimPowerSystems™ modules.

The primary method is to use existing droop control loops within the PowerFactory library to determine the performance of P-f droop control, with the simulation network adapted from [1] and [23] to assess performance in differing network topographies. Analysis will be conducted on the droop controller performance during various situations including changes in load and the loss of generating sources, including the main electrical grid supply. The active voltage and frequency performance will be assessed against the Western Power Technical Rules [11] for network performance; to ensure the droop controller maintains frequency regulation, voltage regulation, and real power sharing is obtained. The objective is to gain an improved viewpoint on the performance aspects of the form of droop control, during both single and parallel operation of the DG units.

Secondarily, the objective is to develop a VSI-based droop controller to integrate within the simulation network platforms to compare. This involves a deeper understanding of the PowerFactory software and is included to expand on the author's knowledge on the use. Simulink software will be used to develop a droop controller for import into PowerFactory, but this will be limited to initial analysis and simulations that are not contained within this report, as they are for development purposes only.

4.1 DIgSILENT PowerFactory™

DIgSILENT PowerFactory™ is an extremely useful computer aided engineering tool that can be used for the analysis of transmission, distribution, and industrial

electrical power systems. This was used as the basis for modelling and simulation activities outlined in this report, due to its interactive ability and dedication to electrical power system and control analysis [27].

The simulation method used was based on the Root Mean Square (RMS) simulation, which considers the dynamics in electromechanical, control and thermal devices in symmetrical operation [20]. The ability to use built-in models for the SG control enabled effects of droop control to be investigated through primary (governor) and secondary (P-f) control. It is recommended that this software program is used further in the analysis of microgrid control, to benefit future students and researchers.

4.2 MathWorks MATLAB / Simulink /Simscape™ / SimPowerSystems™

Simulink, including the Simscape™ and SimPowerSystems™ modules enables the modelling of power distribution network similar to PowerFactory™. For this thesis project report limited use of Simulink was conducted, and only included modelling and investigations conducted when access to PowerFactory™ was limited. This was a very helpful tool in conducting the analysis and has been used extensively in similar studies conducted in the Microgrid control as highlighted in [1], [6], [12] and [16]. Further analysis using this simulation software is warranted but the use of PowerFactory™ is recommended.

4.3 The Diesel Generator

4.3.1 Diesel-Generator Physical Description

The basic structure of a diesel-generator includes both the motor and the synchronous generator, as shown in Figure 12, with the governor control affecting the quantity of fuel supplied to the motor though the fuel valve shown, which then is converted to mechanical power via the clutch. This mechanical power is then converted to electrical (active) power to the diesel-generator busbar for supply to the microgrid. The Automatic Voltage Regulator (AVR) provides the system excitation providing the reactive power [21], but is not discussed further in this report, as this is outside the scope of the investigation.

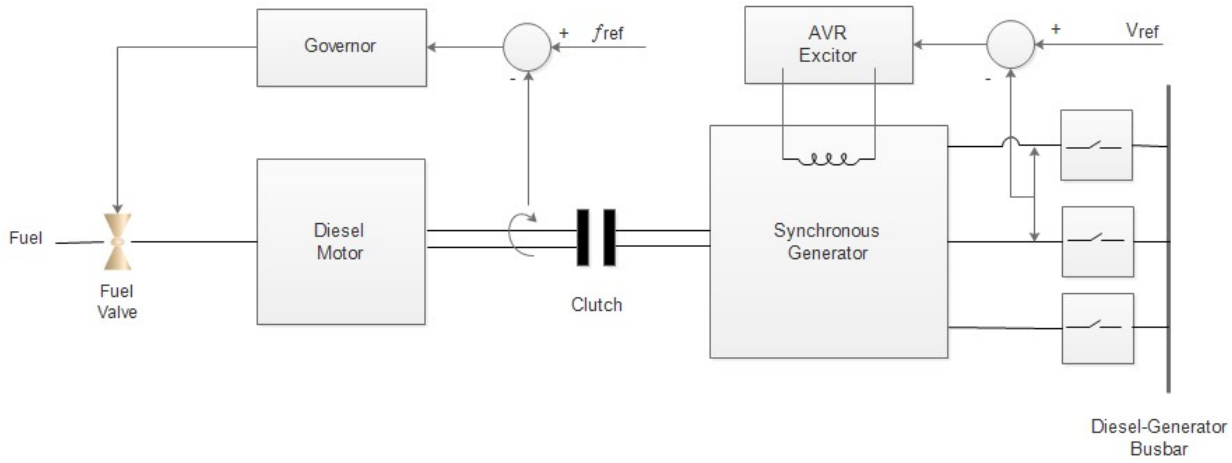

Figure 12: Diesel Generator Structure [28].

This form of generation is commonplace and is a reliable source of power, provided that fuel is available. The governor is required to regulate fuel supplied to the motor to adjust the fuel throttle valve to compensate for differing load demands [21], and will be simulated initially without this form of control to show a comparison on the SG performance.

4.4 Synchronous Generator within PowerFactory

The synchronous generator (SG) used in this thesis is a built-in model within the PowerFactory™ global library (ElmSym), and is representative of a typical SG. It is easy to enter the required parameter settings and generator ratings through the edit dialog once the model has been placed within the grid network frame [20]. The generators used for this thesis have various rating values and have been input manually based on system information provided in [1].

4.5 Diesel Governor Model in PowerFactory

The governor selected in PowerFactory™ is listed as 'DEGOV1' [27], as shown in Figure 13, and is available under the standard models tab within the global library. The model is based on an IEEE model that was developed by the Woodward Company [20].

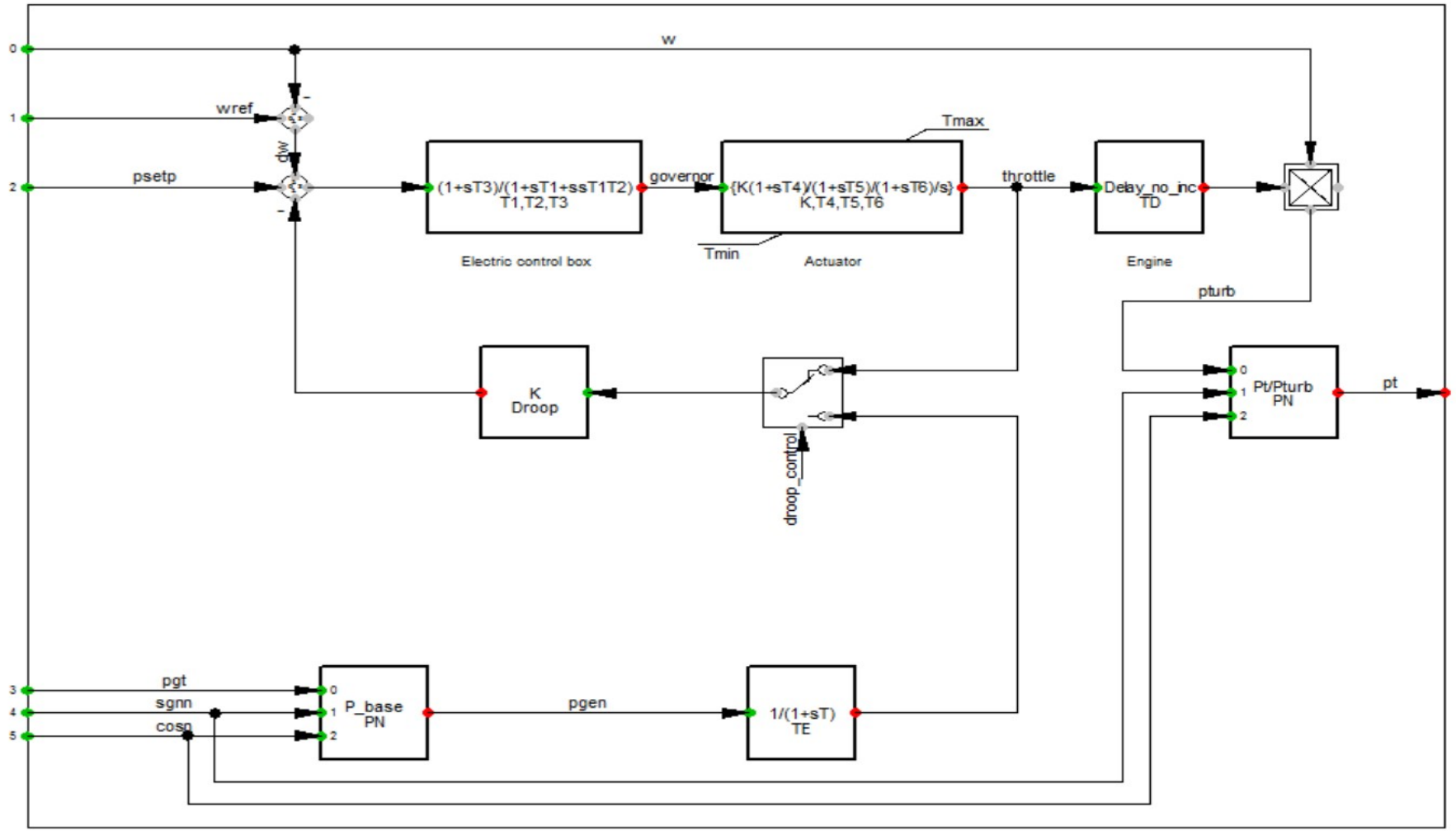

Figure 13: Governor Model [27].

The three main blocks in the model include the electric control box, which is an analogue controller that provides the control signal. The actuator block converts this control signal into a signal to the fuel throttle, adjusting the flow rate to the motor. The engine block models the delay to allow for the time the fuel takes to combust and convert the supplied fuel into a torque signal [20].

The droop characteristics can be adjusted via the parameter settings of the model to simulate the diesel engine performance.

For this thesis investigation, the parameter settings for the simulations conducted were first established based on [20] and [21], before being adjusted to tune the controller to achieve optimum performance and a reduction in droop characteristics. The tuning of the control parameters was achieved through trial and error, given the mathematical methods being complicated for complex paths of control signals [21], and is shown in **Error! Reference source not found.** of Appendix B.

4.6 Voltage Controller in PowerFactory

The AVR used is based on the 1968 IEEE Type 1 [27] within the global library of PowerFactory™, and is shown in Figure 14. This provides the excitation system to the generator by adjusting the excitation voltage of the rotor windings; thereby affecting the reactive power supplied which then impacts on the supply voltage.

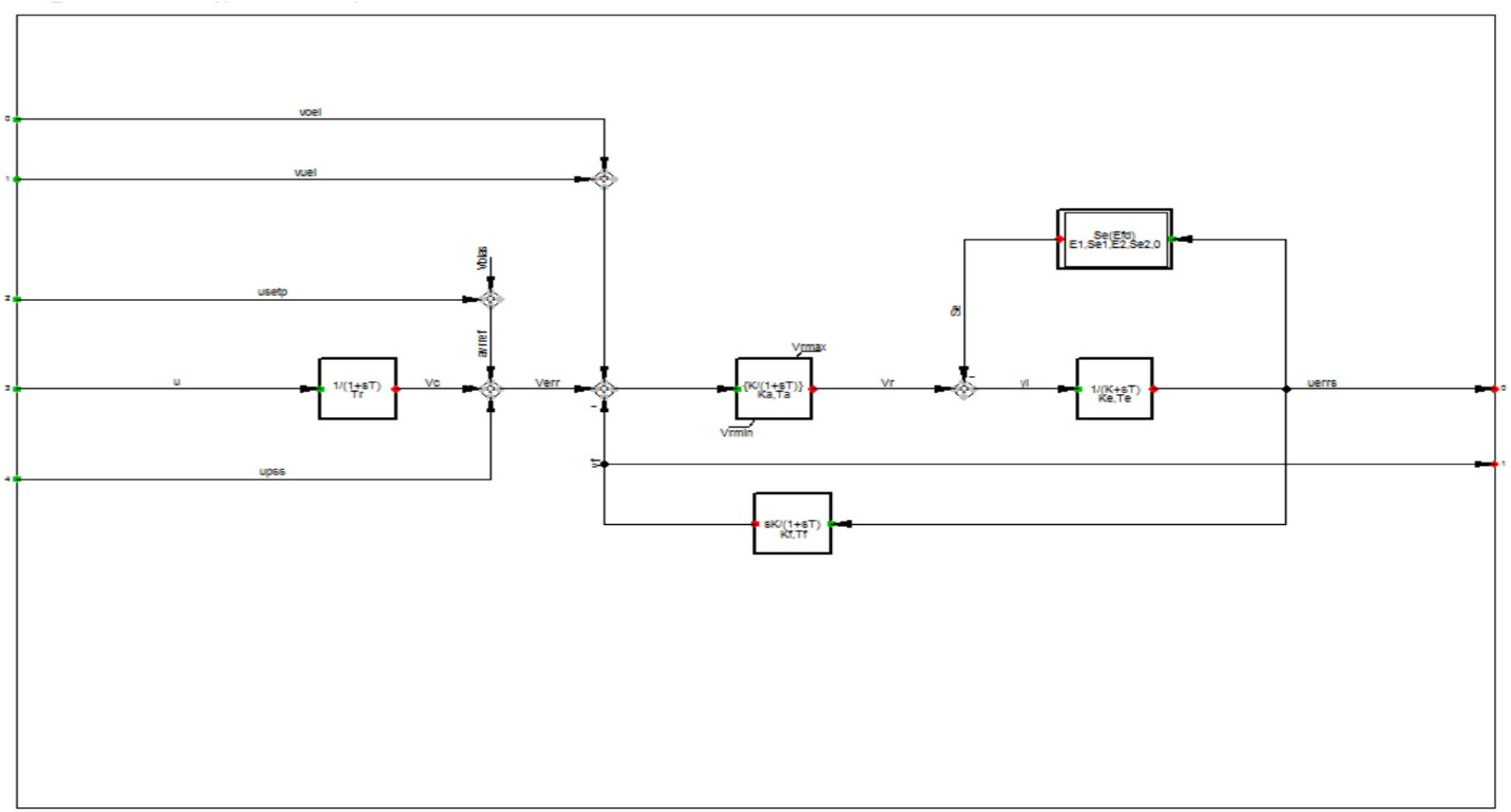

Figure 14: Automatic Voltage Regulator [15].

The voltage regulator used is not investigated further within this thesis but is required to run simulations for the purpose of investigating primary and secondary control. The parameters used for setting up the AVR are contained within Table 5 of Appendix B.

4.7 Power-Frequency Control in PowerFactory

Additionally to the primary control established through the use of the governor and AVR, a secondary (supplementary) controller is implemented for power-frequency control as shown in Figure 15. This has been based on models within [27] to improve power-frequency performance. No parameters were required for this model as it is tuned within the PowerFactory™ software package.

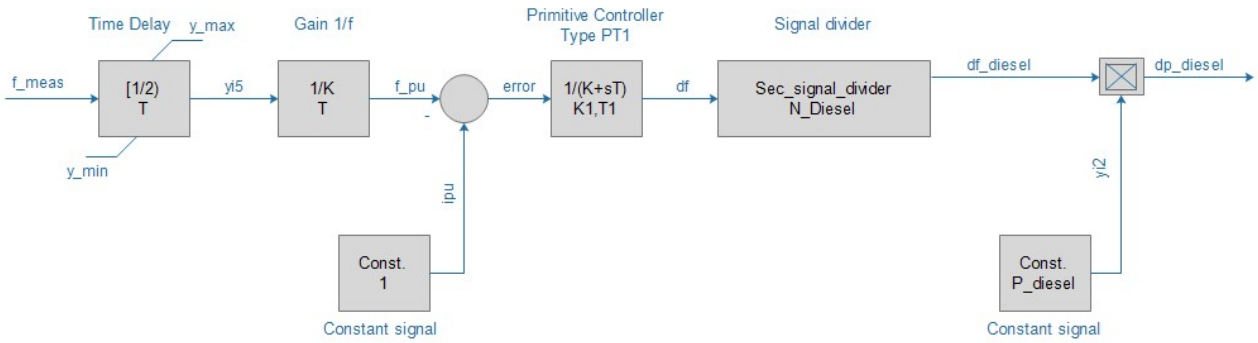

Figure 15: Power-Frequency Secondary Controller [15].

4.8 Power-frequency control in Simulink SimPowerSystems

This model was created in Simulink, to investigate the importing of external models into PowerFactory. It is shown in Figure 16, based on the model developed in [23]. The use of this model was primarily for droop control simulations conducted with Simulink to assess performance but this thesis is based on the PowerFactory software and further investigation is required to implement in a Microgrid network such as Figure 19.

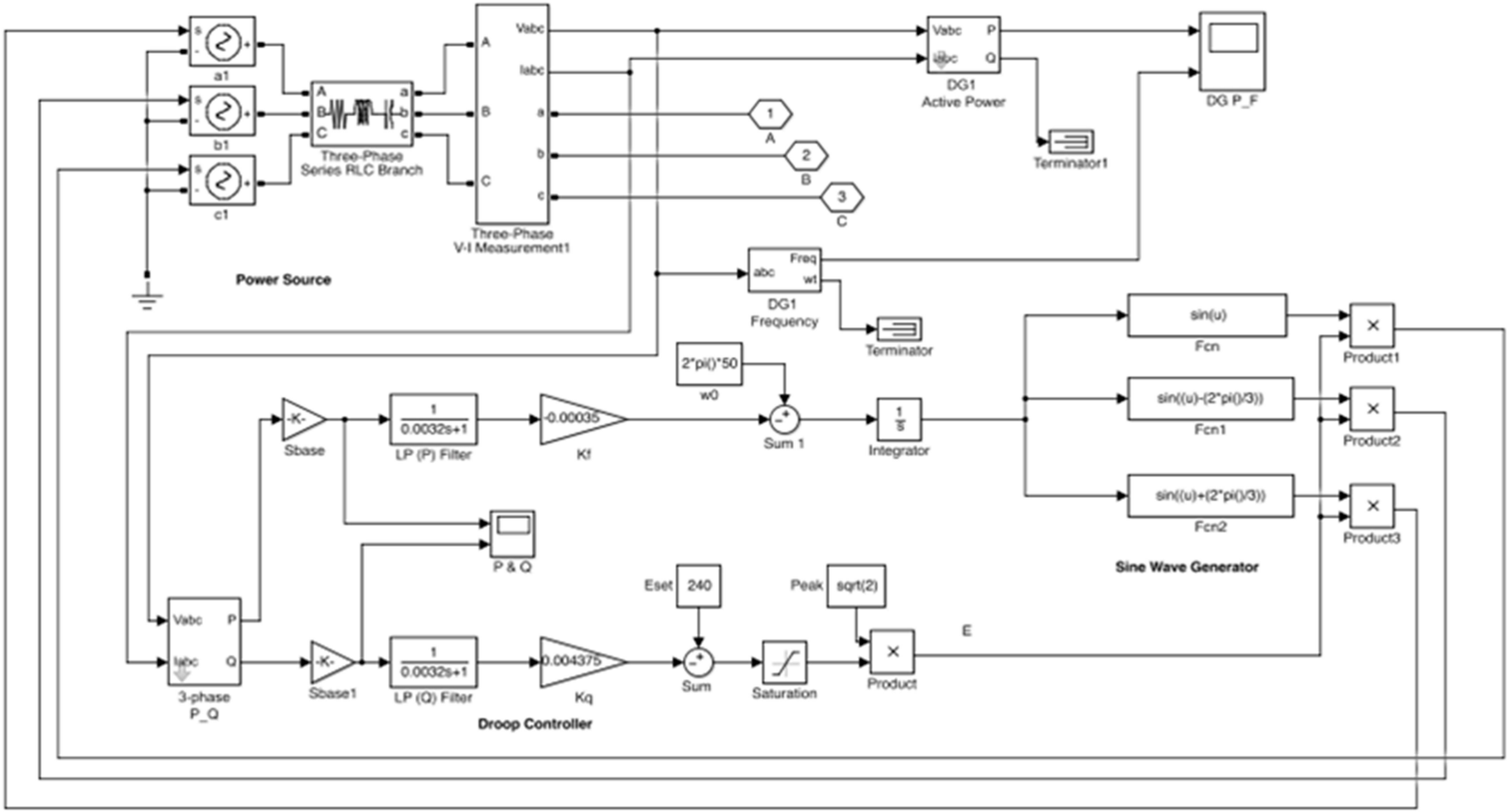

Figure 16: P-Q (P-f) based droop controller in Simulink

This model includes the use of a three-phase supply, controlled by a power-frequency controller and output through a sine-wave generator for supply to the microgrid. The parameters used, are based on the expected frequency in radians per seconds, and the gain settings for frequency and voltage. Additionally, the use of low-pass filters and saturation were included to the control the output voltage and frequency. Whilst this model functional, its implementation in PowerFactory™ was not refined and therefore was not used for simulations. It is included for future reference.

4.9 VSI-based power-frequency droop control

The droop controller developed for a VSI-based simulation is shown in Figure 17, but was unable to be implemented during this thesis, and is included as a basis for further work into the use of slots and the synchronous generator frame [20]. The model is based on [29] with further information available from [30].

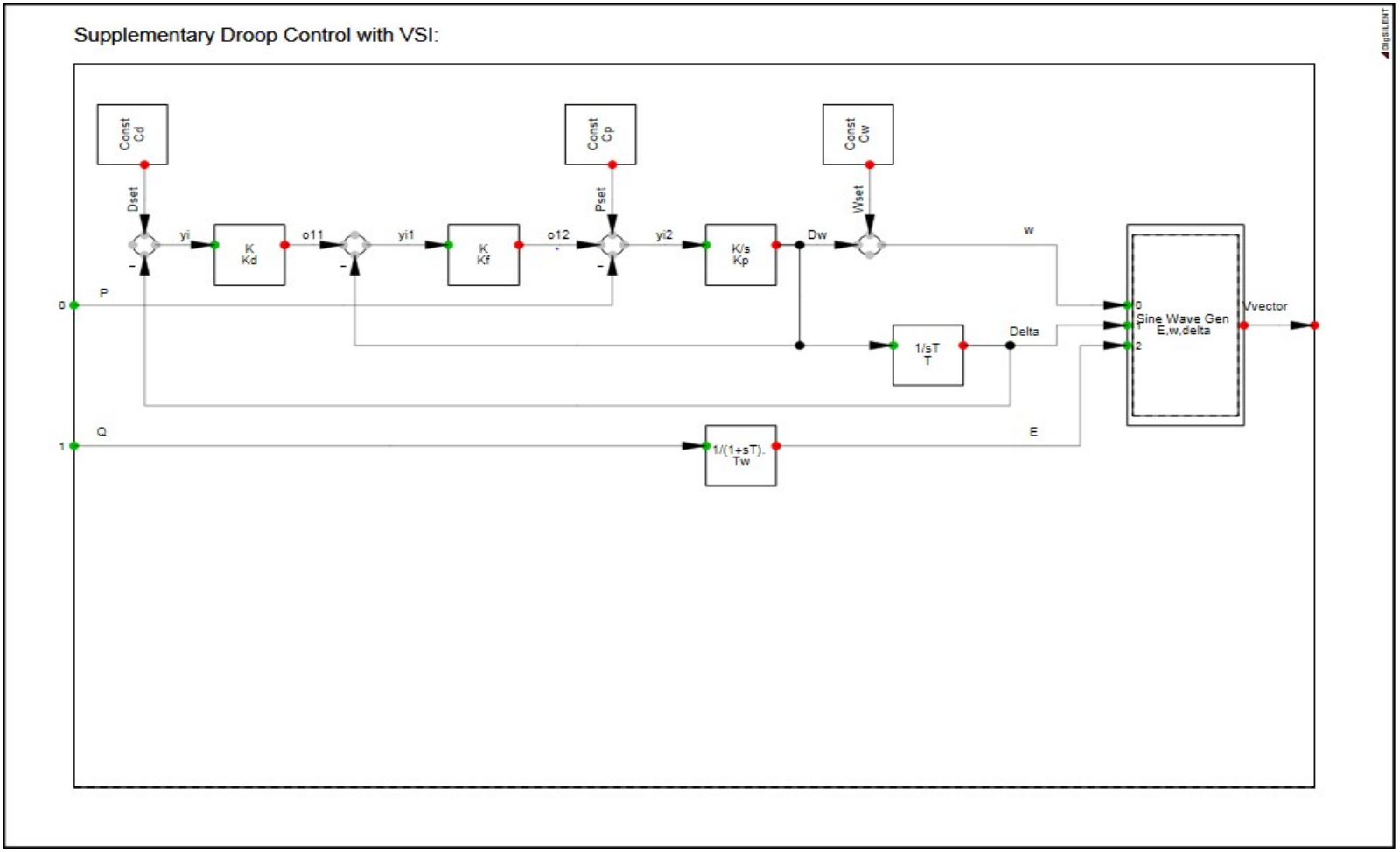

Figure 17: VSI-based P-f droop controller common model

4.10 Model of the Simulation Platform

Two different network configuration were used based on [1], but with a 50 Hz frequency base.

4.10.1 2DG Network Model - Islanded

The performance characteristics during typical load changes were investigated using a simple two DG network using SG models from PowerFactory, as shown in Figure 18. The DGs were rated at 0.6MVA and configured to operate at 4.14kV, stepped up to 13.8kV to replicate a MV distribution line. Both generators have independent local loads and the common load was increased at a set time to determine the active power and frequency response. The parameters used for setting up the simulation were taken from [1] and are included, with minor modifications conducted through trial and error to adapt to the 50 Hz network. The use of the shunt capacitor was also included to support voltage regulation at the common load point. The implemented model within PowerFactory is shown in Appendix C, Figure 40, for reference.

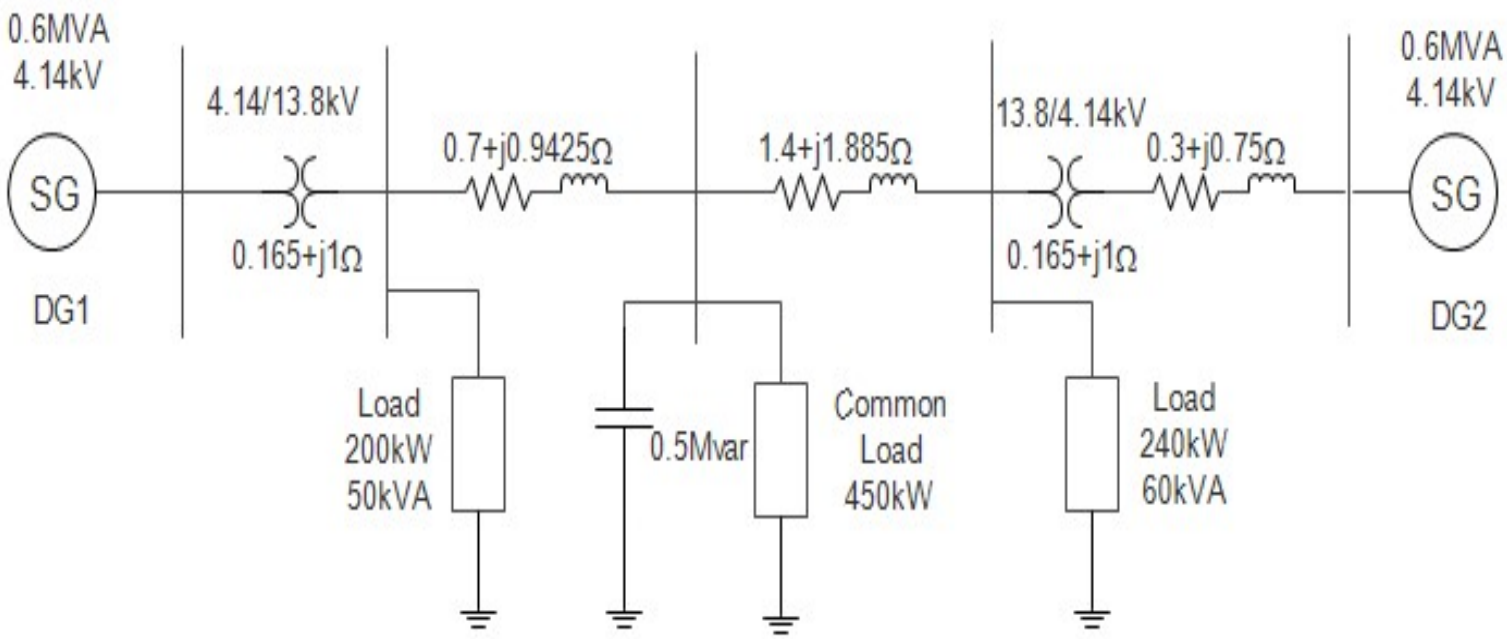

Figure 18: 2DG Model [1].

4.10.2 3DG Network Model – Grid Connected

The larger network shown in Figure 19 [1], shows the microgrid connected to the main electricity grid and is used to simulate not only load changes, but also the loss of grid power and common load impacts. It consists of three distributed generation (DG) systems, in this case SG units, running through transformers that convert the voltage to a value suitable for distribution on a MV network. Local loads are provided for each generator and a common load is included to represent industrial loads. The model implemented within PowerFactory is shown in Appendix C, Figure 41.

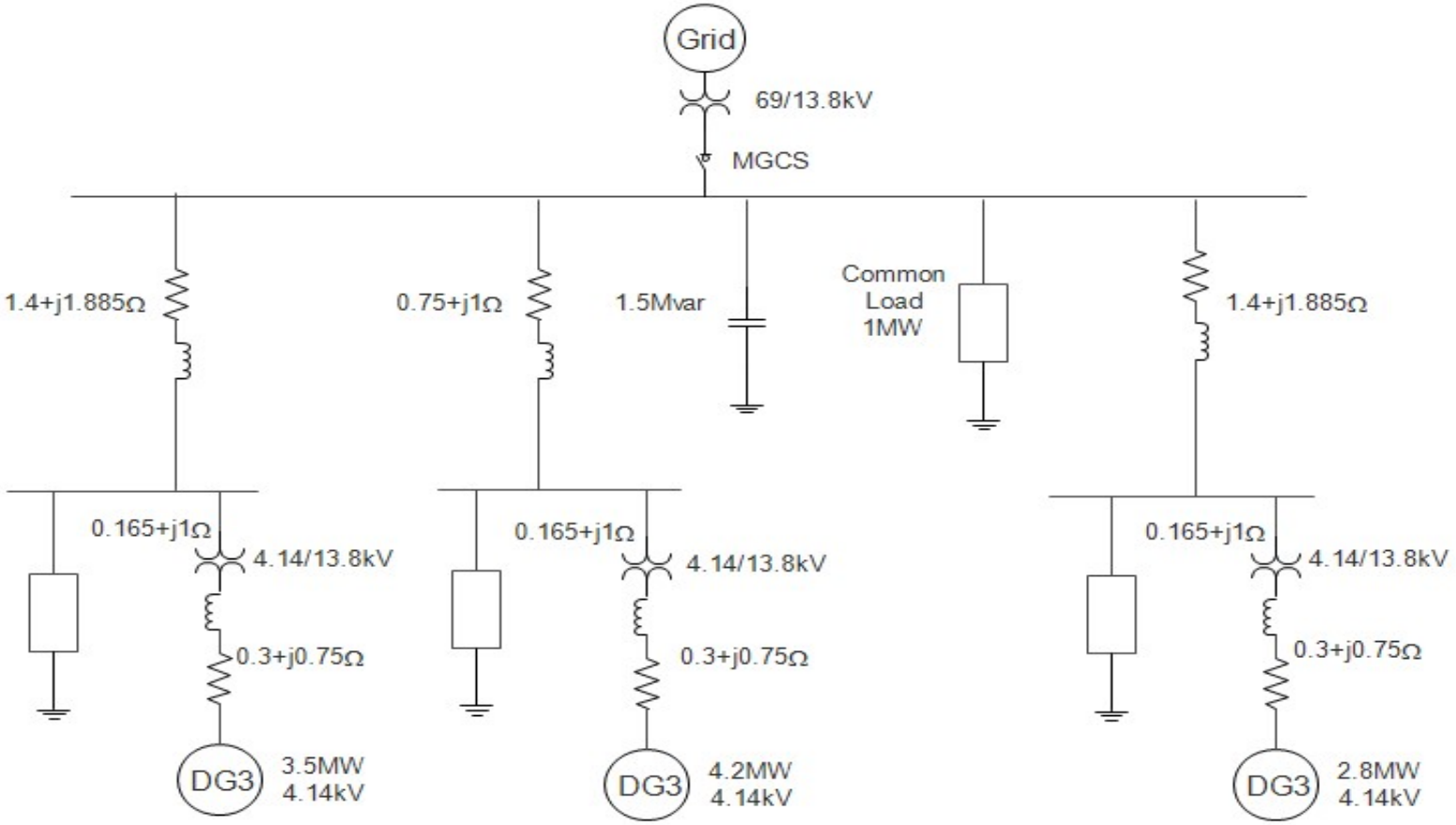

Figure 19: 3DG Network [1].

4.10.3 Single DG network in Simulink

The network shown in Figure 20 was developed to simulate a simple single DG network that is connected to the main electricity grid, and is based on a microgrid network in [23]. It was used to test the VSI-based droop control prior to importing it into PowerFactory™ for use in the larger network shown in Figure 19 above. Further analysis could be done in Simulink with the P-f droop controller developed in section 4.8 based on the use of Simulink as the primary simulation tool, but this is not within the scope of this thesis, as this analysis is supported by many other papers.

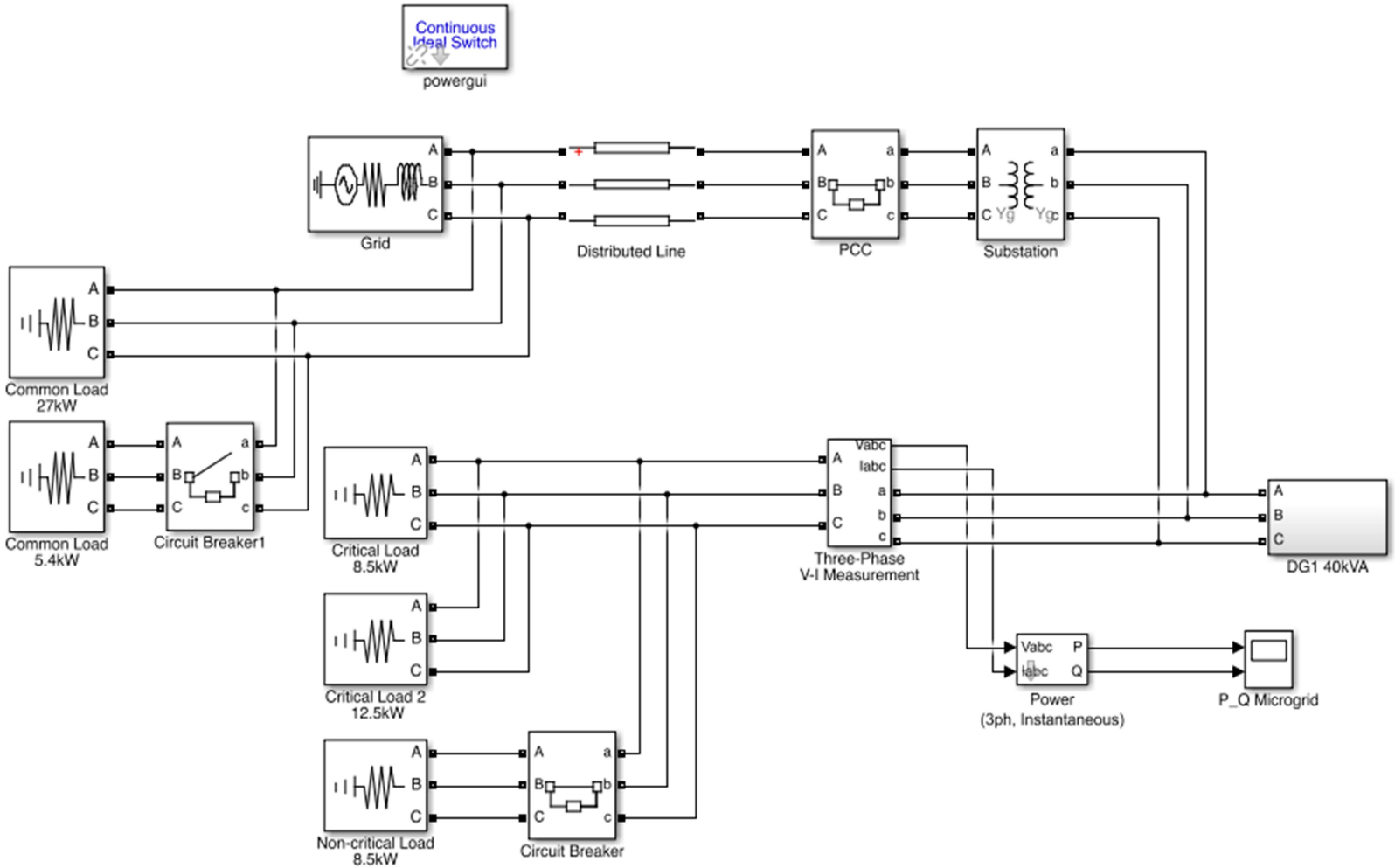

Figure 20: Single DG grid-connected network in Simulink

The network consists of a single DG unit connected to the grid through a substation transformer. The grid side of the network has a common load which can be adjusted to either increase or decrease the load through a switch, with the PCC used to isolate the microgrid to operate in islanded mode. The microgrid has three local loads, two being critical, and one being no-critical so load shedding/load increase can be simulated. This network could be expanded to use renewable resources, but for ease a DG unit is used as a representative generator.

Chapter 5

5 Simulations & Analysis

The purpose of these simulations is to determine the response time taken for the DG to return to a steady-state active power (P) and frequency. The required standard states that the frequency is to remain within the range defined in [11] for grid-connected mode, and when the microgrid needs to re-connect to the grid. A summary of the frequency restriction listed in Appendix A.

In Figure 21 the top plot shows, DG1 active power response followed by DG1 frequency response, DG2 active power response, and DG2 frequency response. For the 3DG network, the same format is applied to the third DG unit.

5.1 Two DG Network

Simulations were run using the 2DG network configuration, Figure 40, to determine the impact of a common load change with no control, governor, AVR, and power-frequency control.

5.1.1 Simulation 1: No Control

This simulation involves a load increase from 750kW to 824kW (ΔP=74kW giving 10% increase) at t=5 seconds, and was run for 40s given the time taken to achieve steady-state. The DG governor (Figure 13) and AVR (Figure 14) sourced from [27] is used with the parameters defined in Table 4 and Table 5, with the governor and AVR disabled. The purpose of this simulation is to show a baseline of the power and frequency response of a synchronous generator without any form of control, though without governor and AVR control it is unlikely the SG would be beneficial to the network.

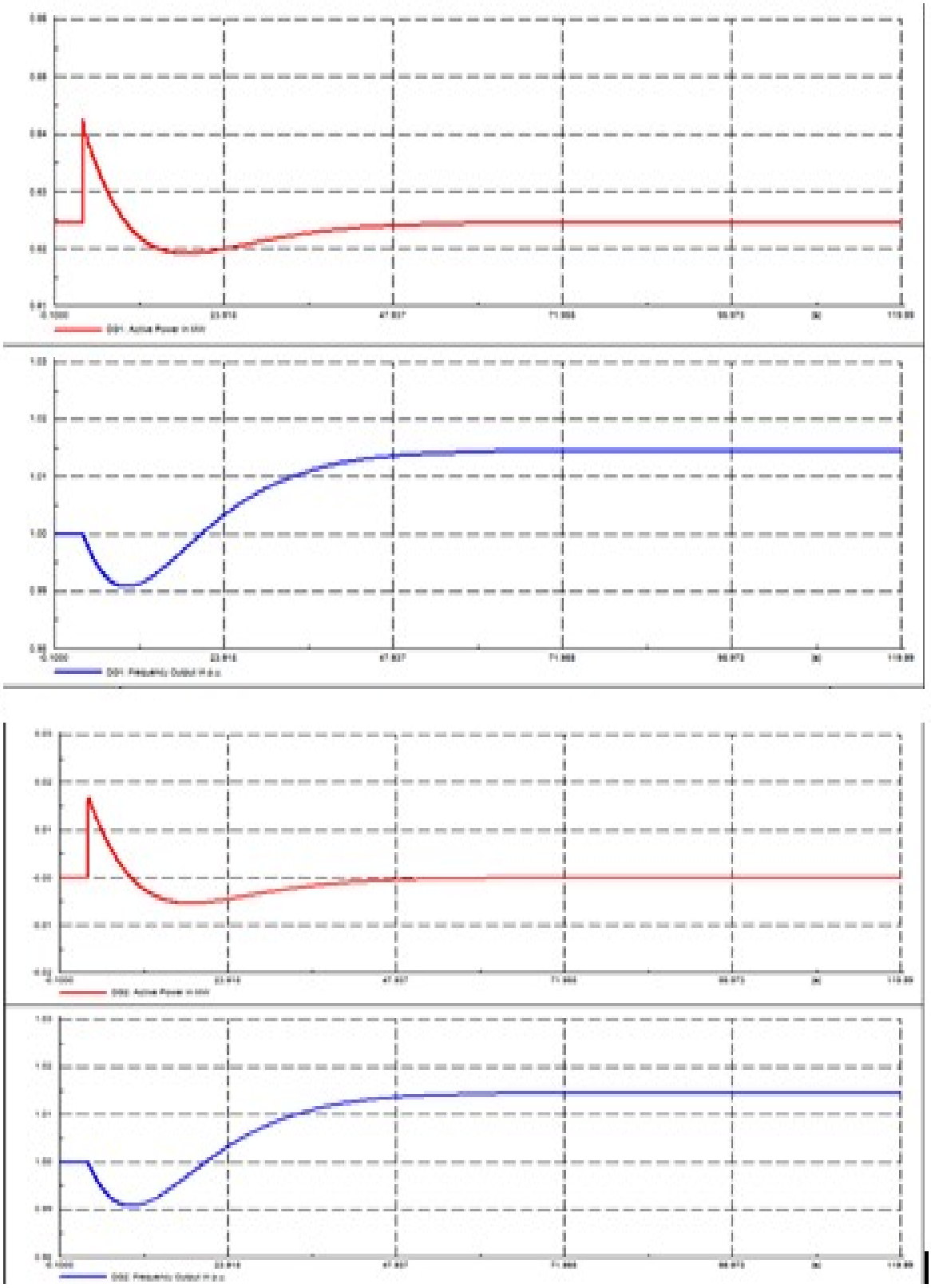

Figure 21: DG1 & DG2 Power-frequency responses.

Figure 21 shows the active power for DG1 shows a peak in output power of ~20kW when subject to a load change, prior to dipping to revert to steady state

active power, taking ~45s for this to occur. The plot highlights how the active power (red line) peaks with the sudden load increase, and then dips before reaching steady state value with a reduction in active power. The frequency response (blue line) shows the droop down to 0.9979pu (49.89 Hz) which is within the guidelines [11] for a grid connected unit, though overshoots to above 1.014pu (50.70Hz) which is outside the limits [11] and would therefore be excluded from connection to the main grid by the MGCS. Another problem relates to the time taken to respond being excessive, highlighting the need for some form of dampening which can be provided by frequency droop control. For DG2 a similar response is provided, as expected. No voltage response was obtained for this simulation, due to tuning of the controller being required first.

5.1.2 Simulation 2: Primary Governor, AVR and P-f control

To simulate the DG response when subject to primary and secondary control, the simulations were re-run, using the parameters detailed in Appendix B Table 4 and Table 5. The purpose was to show that with droop control, the active power and frequency response achieve steady-state much earlier, with the undamped behavior reduced and to determine whether this method of control is suitable for connecting to the main electrical grid.

Figure 22 shows an improved response time for both active power and frequency of the DG units, though improvements could be made by tuning the parameters of the governor to reduce the undamped nature of the frequency response. The active power response for DG1 shows an increase in output power of 17.7kW, with a small spike before reaching a steady state value of 642.1kW in ~4s after the load increase. DG1 frequency response shows a droop to 0.9979pu (49.89 Hz) which is within the tolerance for a DG to be connected to the grid. The frequency response also exhibits some undamped behavior with the steady-state value of 0.9996pu (49.98 Hz) after ~14.8s. This is not as much of a concern given the frequency output is within the required guidelines. DG2 exhibits a similar response to DG1 for the frequency response, with the active power response output being at a lower level 17.5kW showing a power share ratio between the two DG units of 98.35:2.65.

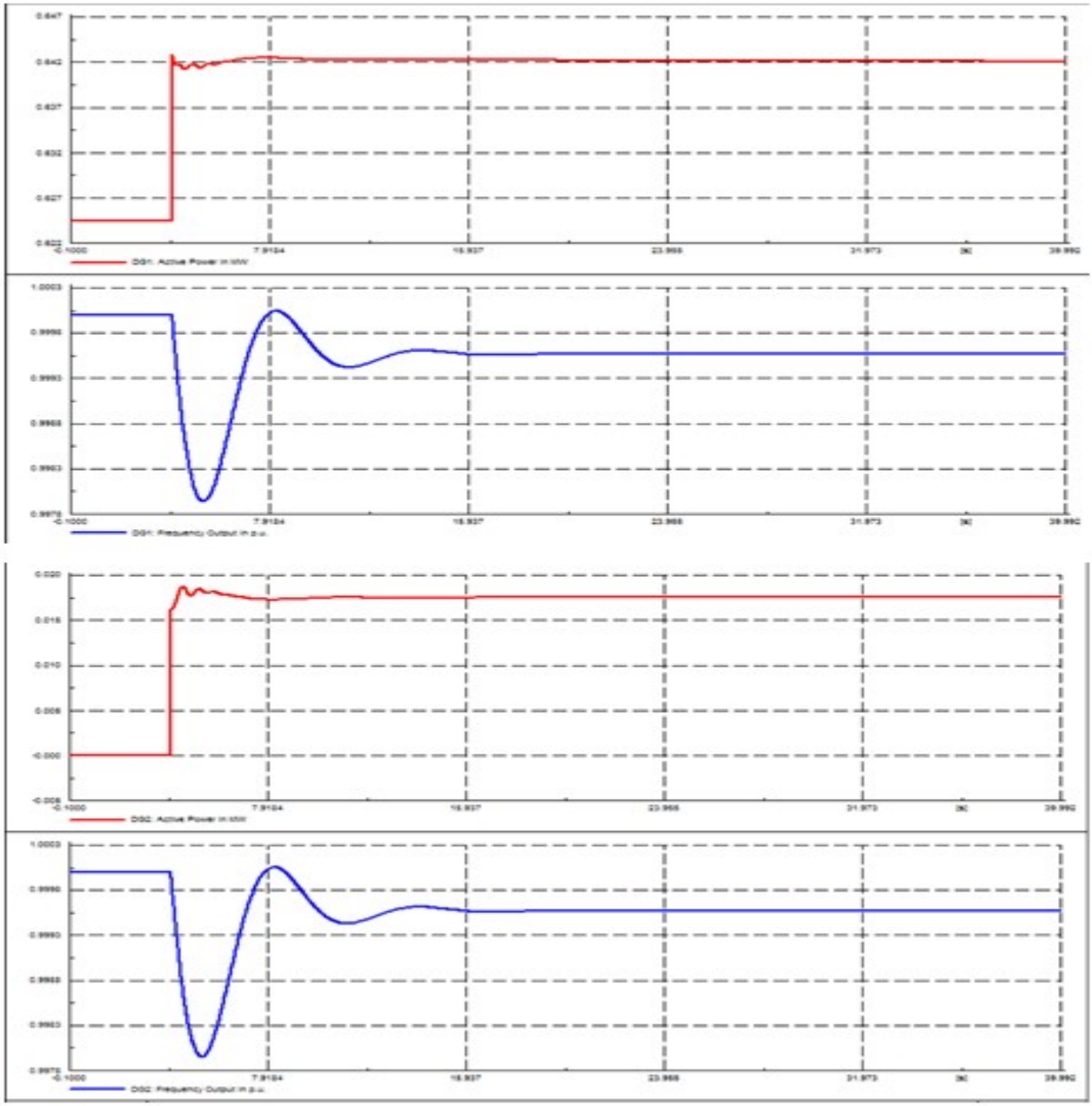

Figure 22 2DG network responses with Governor, AVR and P-f control

To improve performance of the controllers, the governor was tuned using trial and error by increasing the actuator gain (K) to 57 and reducing the actuator derivative time constant (T4) to 0.05s. The rest of the parameters shown in Appendix B Table 4 and Table 5 remained the same. Figure 23 shows the response from the DG1 and DG2 units.

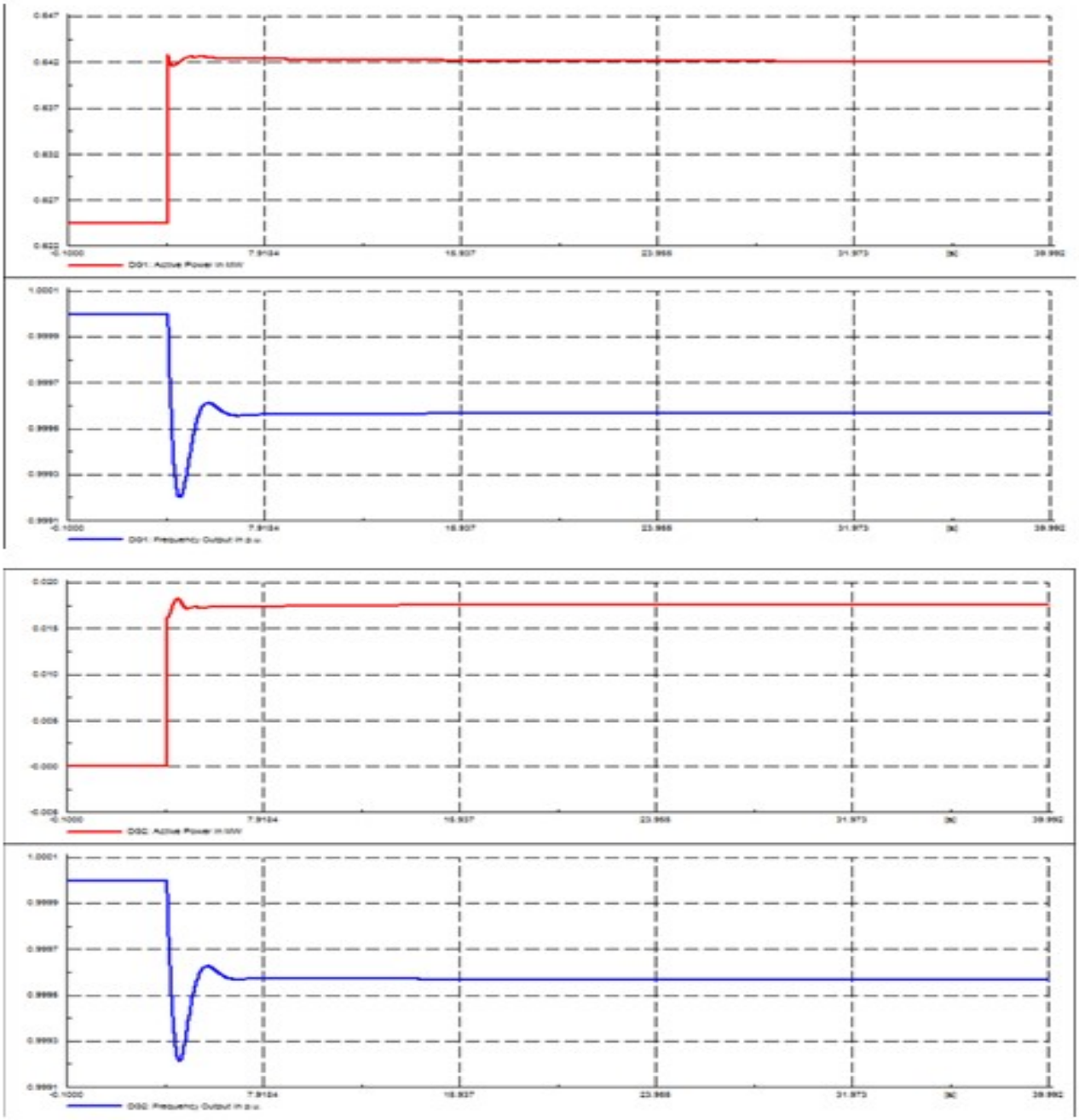

Figure 23: 2DG network power-frequency tuned response

With a more accurately tuned governor, the active power output from DG1 increases by 17.7kW as per the previous simulation, but the frequency output response time has now been reduced. The drop to 0.9992pu (49.96 Hz) is a slight improvement on the 49.89 Hz frequency output during the previous simulation, but the main improvement in DG1 response to the load increase is the time taken to reach steady-state. DG1 frequency achieves steady-state in ~4.2s after the load increase which is an improvement on the 14.8s achieved by the un-tuned controller.

DG2 response is similar with a steady-state active power output of 17.5kW, the same as previous, and a steady-state frequency output of 0.9996pu (49.98 Hz), well within the limits. In summary, it is evident that this form of droop control is sufficient for connection to the main grid.

The voltage regulation of DG1 and DG2 is shown in Figure 24, where for DG1, the voltage changes from 0.9984pu (4.13kV) to 0.9997pu (4.14kV) at t=4s then achieves steady-state of 0.9994pu (4.14kV) 4.7s later. DG2 voltage responds to the common load change with a drop in voltage from 0.9835pu (4.07kV) to 0.9851pu (4.08kV), achieving a steady-state voltage of 0.9846pu 1.3s later. This is within the limitation set by [11], and shown in Appendix A.

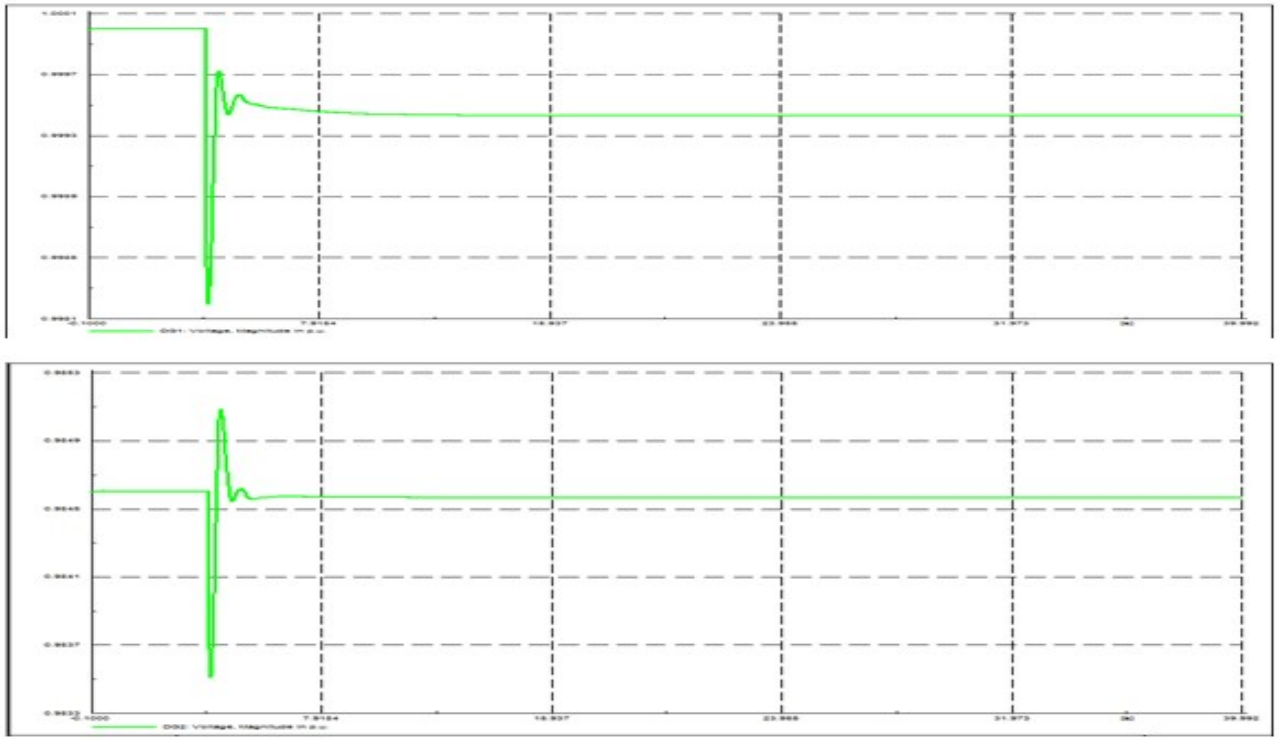

Figure 24: 2DG network voltage response

5.2 3DG Network – Grid connected

Simulations were run using the 3DG network configuration shown in Figure 41, to determine the impact of a grid-disconnect scenario, which is followed by a common load increase to assess the performance of this type of droop controller

with a larger grid-connected network with different size DG units. The simulations consist of scenarios including the microgrid being disconnected from the main grid, loss of a DG unit (possibly due to maintenance) and load increases which could be due to customer demand increase during specific times of the day. The simulation time of 20s is much shorter than a full day profile, but could easily be expanded once a load profile of the area is developed. The DG governor parameters used are shown in Appendix B, Table 4 but with K=57 and T4=0.05s.

5.2.1 Simulation 1: Common load increase

The first simulation using the 3DG grid-connected network shown in Figure 41, involves the microgrid being disconnected from the grid at t=4s and an increase of 250% in the Common Load; 1MW to 2.5MW at t=8 seconds, and run for 20s. This simulation included a power-frequency supplementary controller, with the governor parameters as shown in Appendix A changed. Table 1 shows the simulation events, the type of event, time encountered, and location of the event. Figure 25 shows the active power (upper red line) response and the frequency (lower blue line) response for DG1, DG2, and DG3.

Table 1: Simulation events conducted for load increase scenario

Simulation event	Type	Time (s)	Location
Grid disconnect	Switch event	4	PCC
Common load increase	Load event	8	Common load

5.2.1.1 DG1 response

As shown in Figure 25, the active power output response of DG1 shows the first event at t=4s where the grid is disconnected. It is evident that the DG supply is not required during grid-connected mode as prior to the disconnect event no active power was produced for use of the microgrid. Upon grid-disconnect, the DG1 power increased to just under 2MW, then after the load event at t=8s the output power increased to just over 2MW. The frequency response shows a drop to 0.9807pu (49.0 Hz) before reaching a steady-state of 0.9884pu (49.4 Hz) after 4.0s. Whilst the frequency output is now outside the limits defined in Appendix A,

for a grid connected unit, and that of an islanded unit, it is above the lower limit set for a 2-event scenario which is 47.0 Hz.

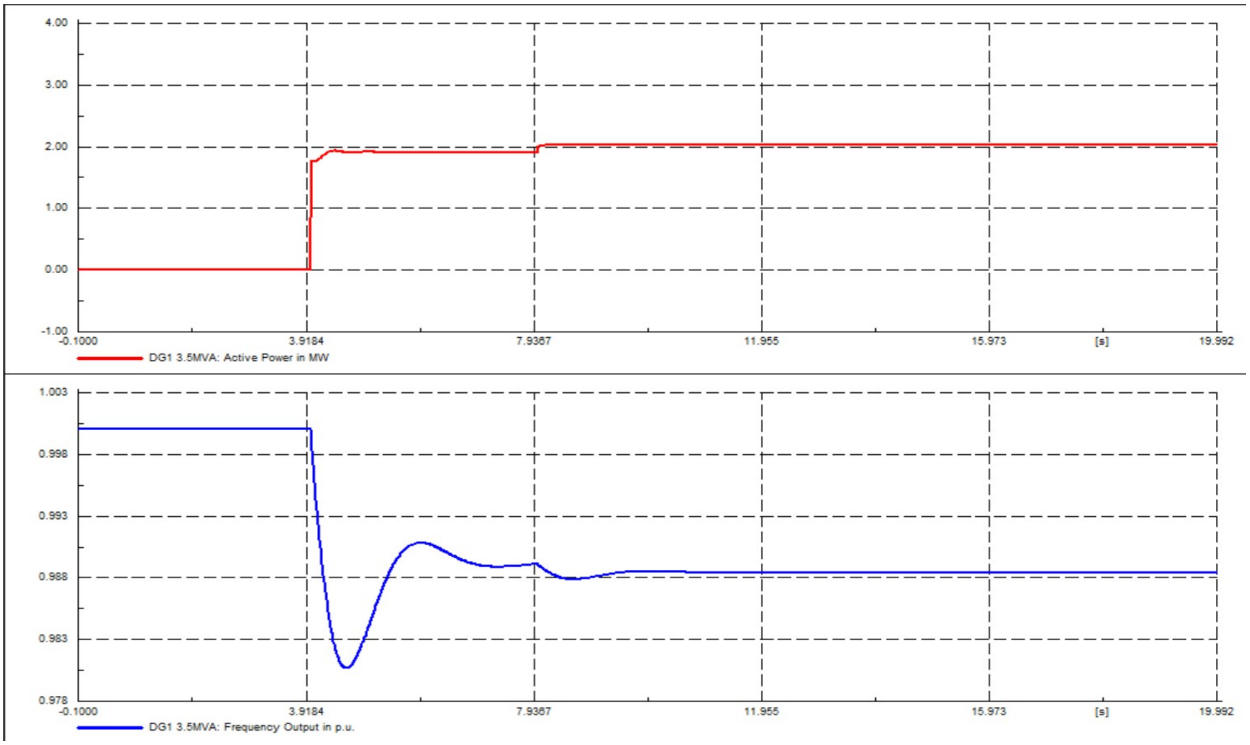

Figure 25: DG1 power-frequency response

The voltage response shown in Figure 26 of DG1 drops to 0.9506pu (3.94kV) and peaks to 0.9824pu (4.07kV) when the grid disconnects at t=4s, before settling at 0.9754pu (4.04kV). The DG voltage then drops again after the common load increase at t=8s, to 0.9721pu (4.02kV) and peaking at 0.9756pu (4.04kV), before reaching a steady-state voltage output of 0.9734pu (4.03kV) after 7.8s. This is within the limits set by [11], and listed in Appendix A.

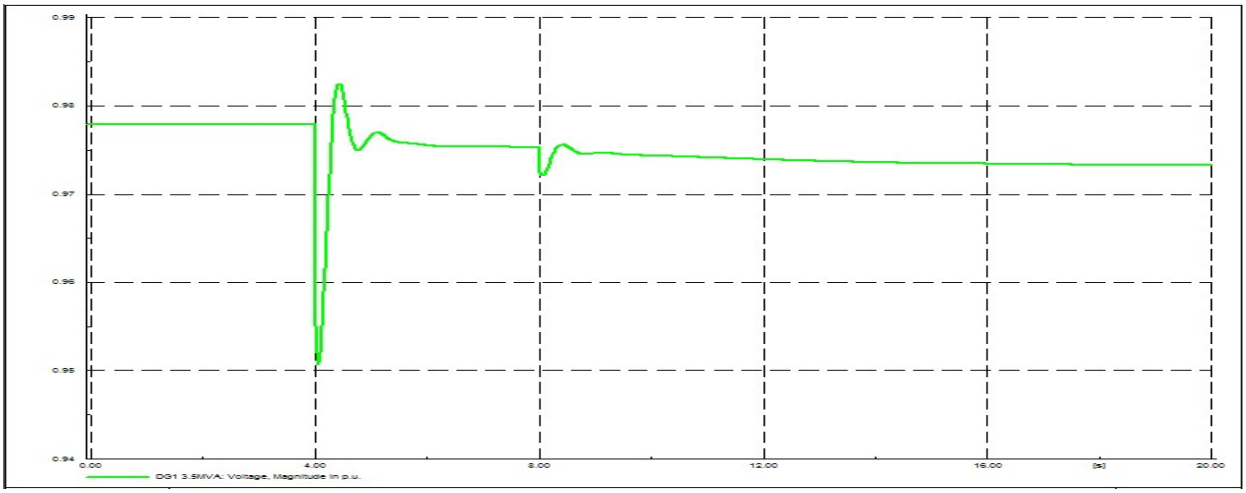

Figure 26: DG1 voltage response

5.2.1.2 DG2 response

DG2 shows an active power response where is now outputs 2.21MW to the microgrid network after the grid-disconnect event, then increase to output 2.37MW after the common load increase, which is to be expected. The frequency response shows a drop to 0.9806pu (49.03 Hz) which is within tolerance for a single event and the subsequent second event at t=8s shows another minor drop prior to the frequency achieving steady-state, which is at ~10s. This shows the controller is acceptable for this DG unit.

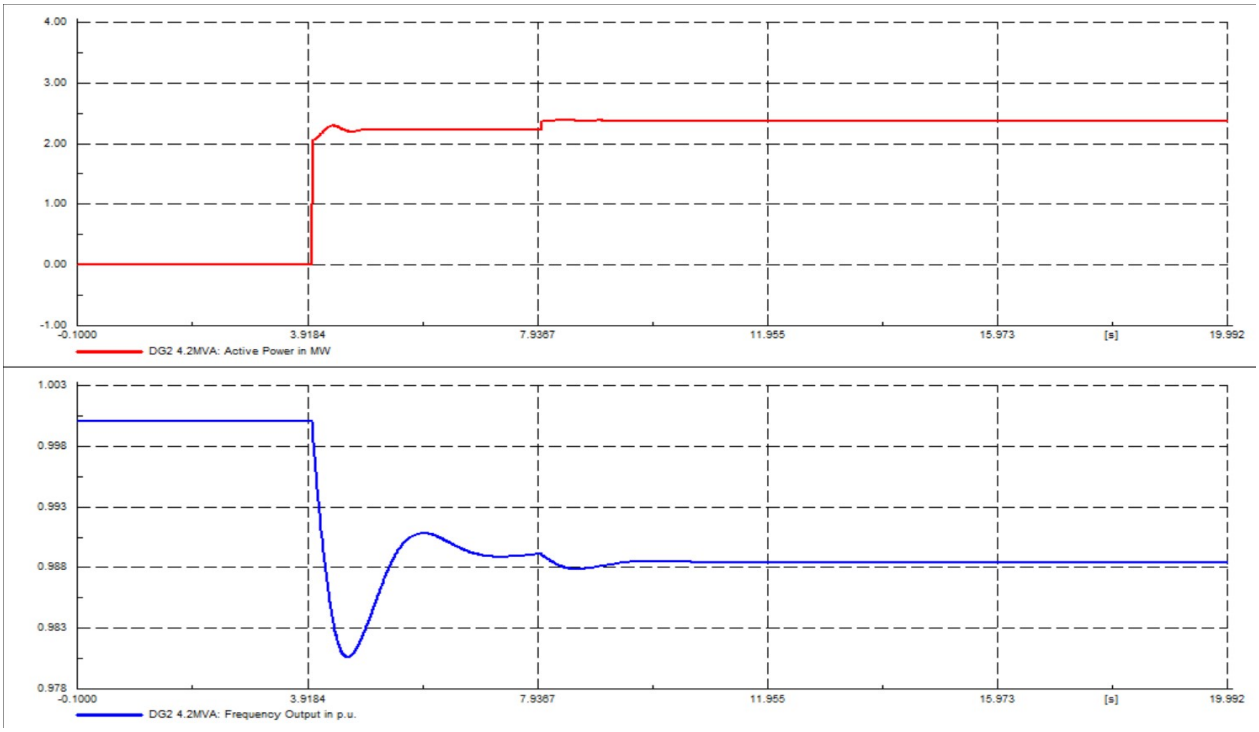

Figure 27: DG2 power-frequency response

The voltage response shown in Figure 28 of DG2 drops to 0.9631pu (3.99kV) and peaks to 0.9836pu (4.11kV) when the grid disconnects at t=4s, before settling at 0.9765pu (4.08kV). DG2 voltage then drops again after the common load increase at t=8s, to 0.9834pu (4.07kV) and peaking at 0.9868pu (4.08kV), before reaching a steady-state voltage output of 0.9846pu (4.08kV) after 7.8s. This is within the limits set by [11], and listed in Appendix A.

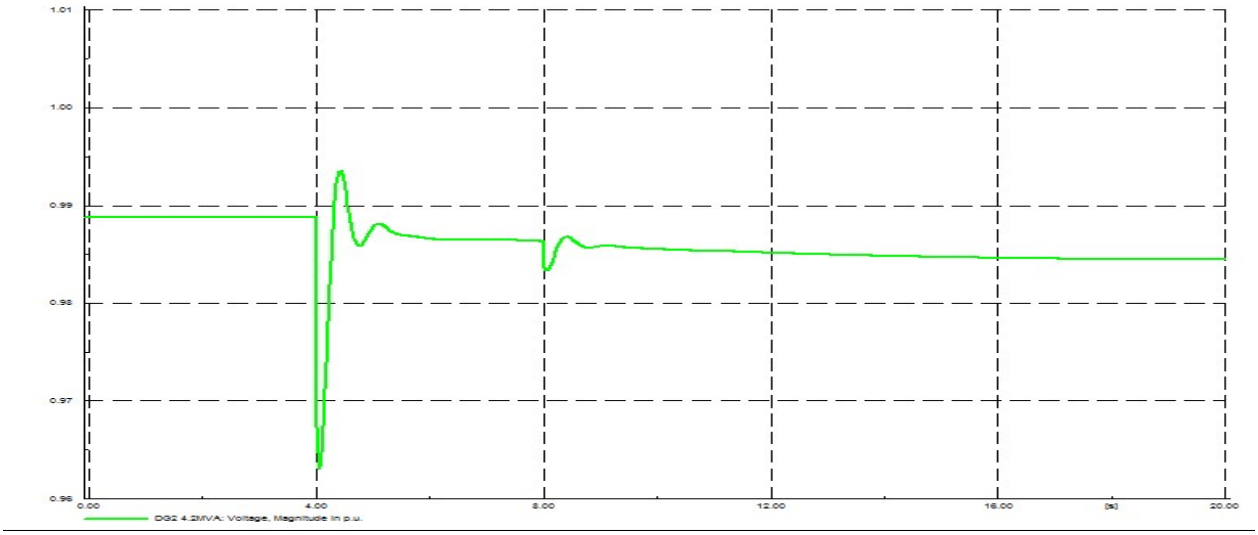

Figure 28: DG2 voltage response

5.2.1.3 DG3 response

DG3 shows a similar active power response with 1.50MW being output to the microgrid, increase to 1.65MW after the second event. The frequency response shows a drop to 0.9810pu (49.05 Hz), exhibiting a similar frequency response to DG1 and DG2 during the grid disconnect and load increase events, and achieving steady-state at 0.9882pu (49.41 Hz), which is within the limits of a 2 event scenario but would need to be improved to meet the limits of a grid-connected DG unit.

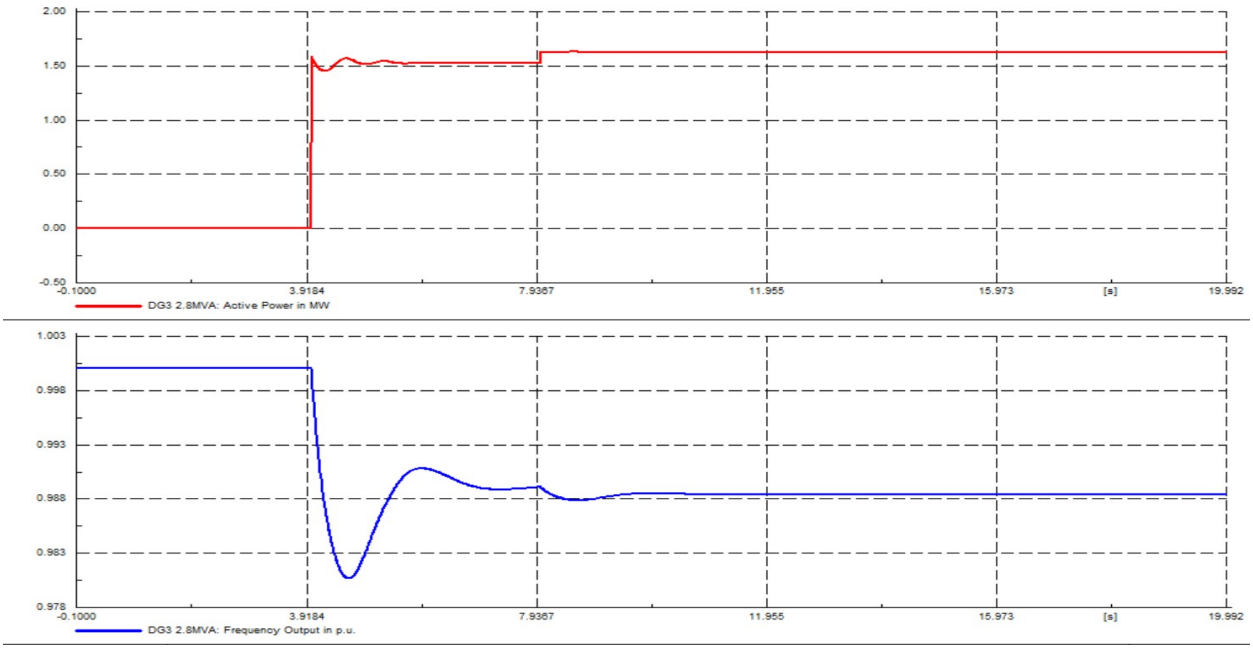

Figure 29: DG3 power-frequency response

The voltage response shown in Figure 30 of DG3 drops to 0.9506pu (3.94kV) and peaks to 0.9866pu (4.08kV) when the grid disconnects at t=4s, before settling at 0.9799pu (4.06kV). DG3 voltage then drops again after the common load increase at t=8s, to 0.9764pu (4.04kV) and peaking at 0.9800pu (4.06kV), before reaching a steady-state voltage output of 0.9780pu (4.05kV) after 7.8s. This is within the limits set by [11], and listed in Appendix A.

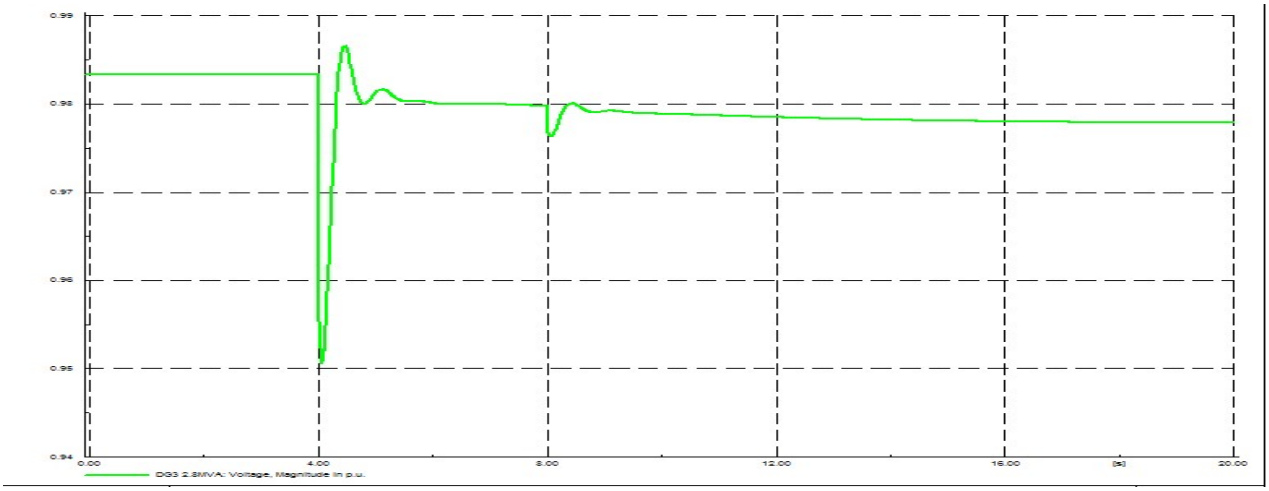

Figure 30: DG3 voltage response

In summary, this type of droop control meets the performance specification defined in [11], though investigation into an alternative controller type is warranted to improve frequency response. Also determination of the category the switching events, defined in Table 3, fall within should be confirmed as voltage regulation requires improvement, during grid-restoration events.

5.2.2 Simulation 2: Grid disconnect/reconnect and load/DG changes

The final simulation conducted was to simulate various events that could occur with a microgrid connected to the main electrical grid. These events were based on simulations conducted in [1], with minor adaptations. The switch and load events conducted are listed in Table 2, including the simulation purpose, type of event, time event occurred and the location within the network. These include scenarios of the microgrid being disconnected and reconnected from to the main grid, temporary loss and restoration of a DG unit, and common load increases.

Table 2: Simulation events conducted for grid disconnect scenario

Simulation event	Type	Time (s)	Location
Grid disconnect	Switch event	4	PCC
DG2 disconnect	Switch event	10	DG2
Common load increase	Load event	16	Common load
DG2 reconnect	Switch event	20	DG2
Grid restoration	Switch event	30	PCC

The power and frequency response for DG1, DG2 and DG3 obtained from this simulation is shown in 5.2.1.1-5.2.1.3. For the power-frequency response plots the upper diagram (red line) shows the active power response, and the lower diagram (blue line) shows the frequency response. The grid-restoration and voltage response plots are shown separately after scaling.

5.2.2.1 DG1 response

As seen in Figure 31, DG1 shows an active power output to the microgrid increase to 1.92MW after the microgrid network is disconnected from the main grid, followed by an increase in power output of 3.08MW. The DG continues to output this value until exposed to the grid-restoration event (Figure 32) with the common load increase of 20% at t=16s having very little impact. After some fluctuation in active power when DG2 is restored the resulting steady-state output power from DG1 is 1.94MW. It is also evident that the spike in power output to 4.73MW is greater than the DG rating, but is transitional so should not pose a problem. The frequency response shows a drop to 0.9807pu (49.0 Hz) after the grid disconnect event, before recovering to just under 0.9900pu (49.5 Hz) prior to the DG2 disconnection at t=10s. It then drops to 0.9781pu (48.9 Hz), then the frequency is restored to 0.9889pu (49.45 Hz) before the DG2 reconnection event occurs at t=20s, where a further drop to 0.9779pu (48.9 Hz) and spike to 1.002pu (50.1 Hz) occurs, and reaching a steady-state frequency of 0.9891pu (49.5 Hz). There was very little impact to DG1 frequency output with the load increase suggesting a larger load increase could be used for future simulations. Given the microgrid frequency was in islanded mode and experienced 2 events, the required limits are between 47.0-52.0 Hz as indicated in Appendix A. The DG1 frequency is maintained within these limits throughout the scenario, though consideration needs be given to assurance of the DG frequency restoration to above 49.8 Hz. Grid (50Hz) restoration is shown in Figure 32, where there are clear oscillations of between -15MW and 15MW for a period of 30s before achieving a steady-state active power output of 0MW (ie. no output), what it was prior to the grid disconnection event. The frequency response for DG1 when reconnected to the grid shows oscillating activity but does not exceed the

frequency limits for this type of scenario and settles to a steady-state frequency of 0.9981pu (49.9 Hz) within an acceptable time of 30s [11].

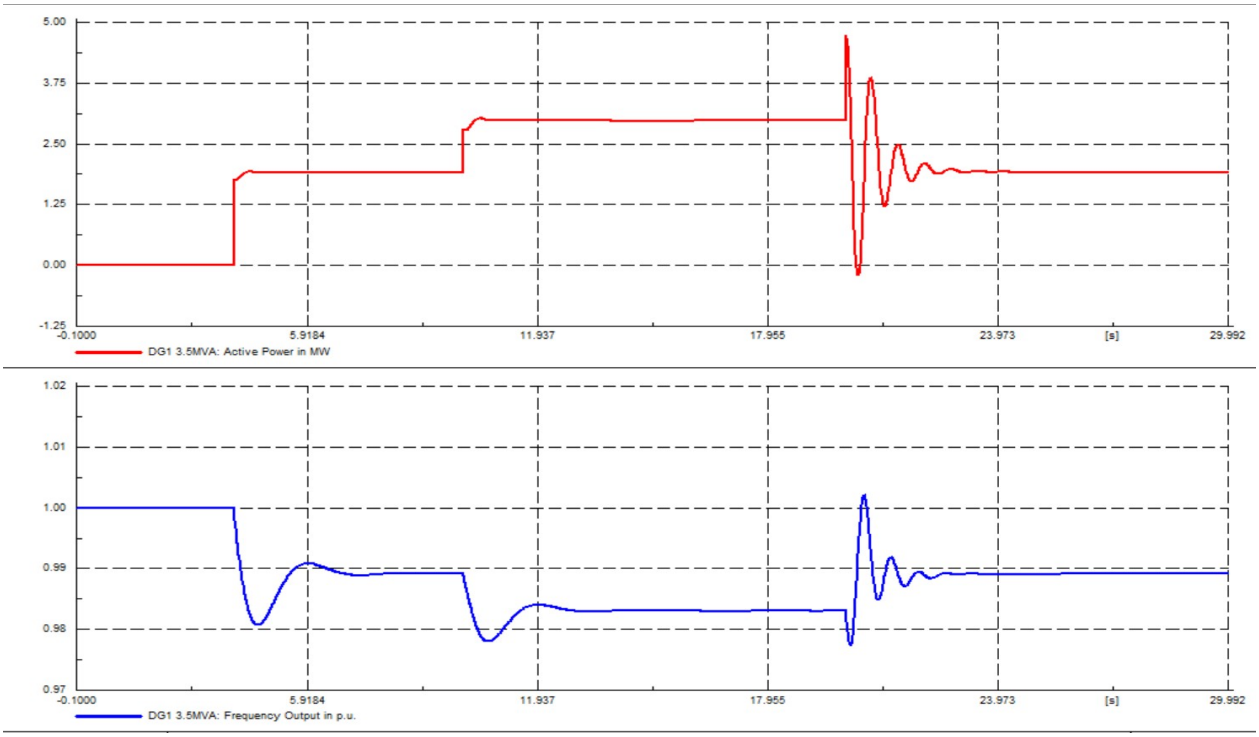

Figure 31: DG1 response

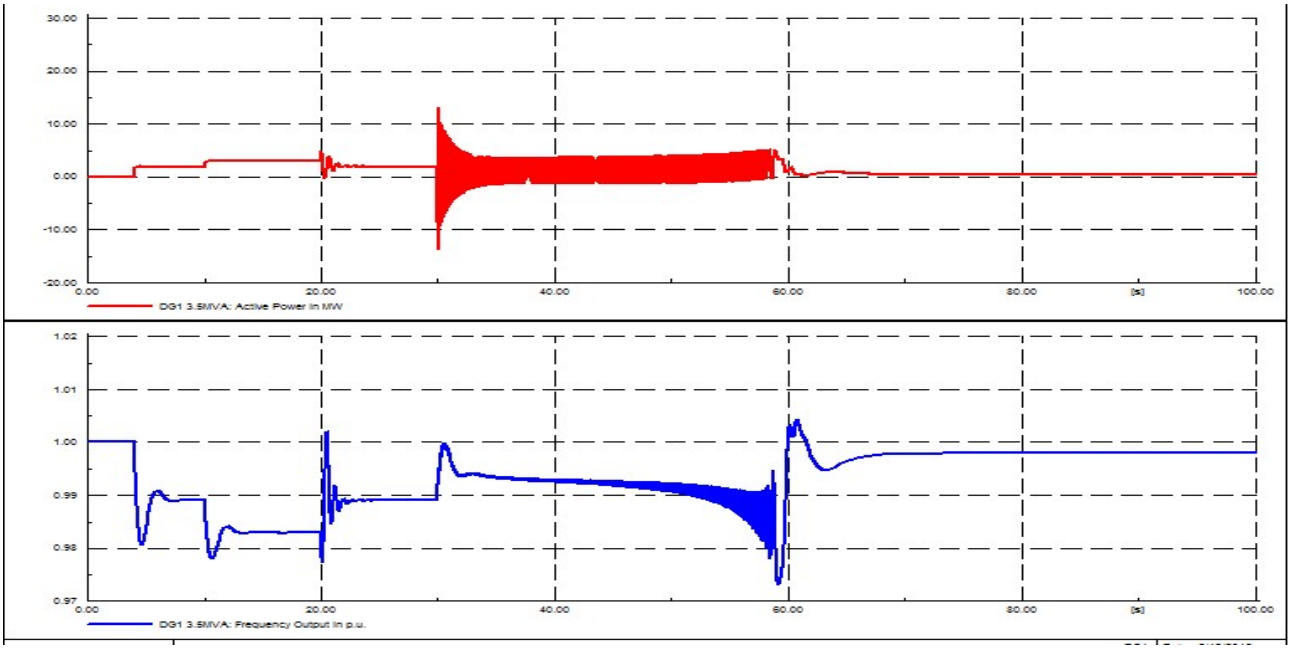

Figure 32: DG1 response to grid-restoration

Voltage regulation for DG1 is shown in Figure 33, where the voltage dips to 0.9507pu (3.94kV) when the grid is disconnected, again to 0.9449pu (4.16kV) when DG2 is disconnected, but return to nominal voltage momentarily. When the load increase occurs, there is minimal impact, and when DG2 is reconnected at t=20s the voltage fluctuates from 0.8775pu (3.86kV) to 1.0360 (4.56kV) before returning to nominal voltage. The greatest impact to the DG voltage output occurs when the main grid is re-connected at t=30 when the fluctuation in output voltage is much more extreme, fluctuating from 0.0428pu (0.19kV) to 1.7635pu (7.76kV) over a period of 38s before achieving steady-state at the nominal voltage. The standard outlined in Appendix A, indicates an allowance of +6% and -10% of nominal voltage. DG2 reconnected causing the DG1 voltage output to be outside these parameters, and at the grid-restoration voltage output is well outside the upper and lower limits, unless this is considered as a consequence of a non-credible contingency event [11]. At steady-state after all switching and loads events are complete, the voltage returns to 0.9779pu (4.05kV), which is within 2.2% of nominal voltage.

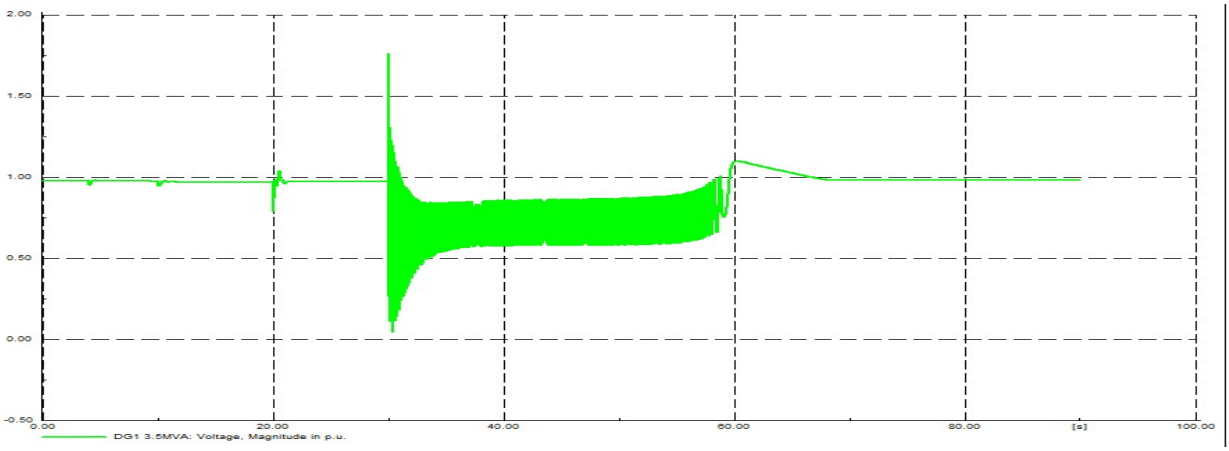

Figure 33: DG1 voltage response

5.2.2.2 DG2 response

DG2s active power response as shown in Figure 34, shows an output power of just under 2.5MW when the main grid is disconnected and then dropping to zero when the DG unit is disconnected, as expected. When reconnected at t=20s, the active power becomes negative prior to increasing to a peak of 6.3MW, oscillates and then reaches a steady-state value of just under 2.5MW after 4s from the

switch event. This remains steady until the grid is restored. Figure 35 shows that DG2 experiences oscillations with peak power of 15MW before settling back to 0MW after 30s, which is what the DG output was prior to grid disconnection. The frequency response shows the drop to 0.9822pu (49.1 Hz) when the main grid is disconnected before recovering to 0.9838pu (49.2 Hz). When the DG is disconnected, the frequency reverts to its nominal 50 Hz until it is reconnected at t=20s. Here the frequency output from the DG undertakes a spike and then drops to 0.9789pu (48.9 Hz) before achieving steady-state frequency of 0.9837pu (49.2 Hz). The DG continues to output at this frequency until the main grid is restored and it then oscillates ranging from 1.0069pu (50.3 Hz) down to 0.9750pu (48.7 Hz) and settles at a frequency of 0.9979pu (49.9 Hz) within 40s, well within the required time of 15 minutes for under-frequency above 48.5 Hz [11].

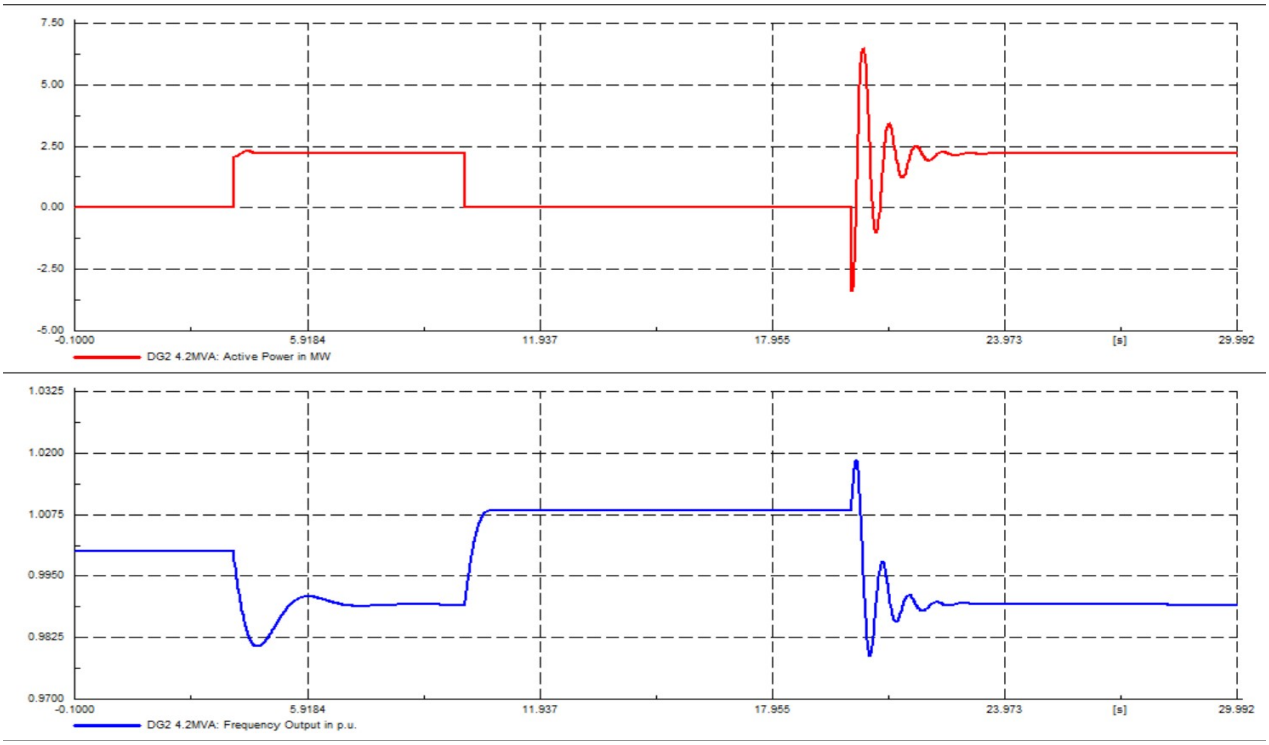

Figure 34: DG2 power-frequency response

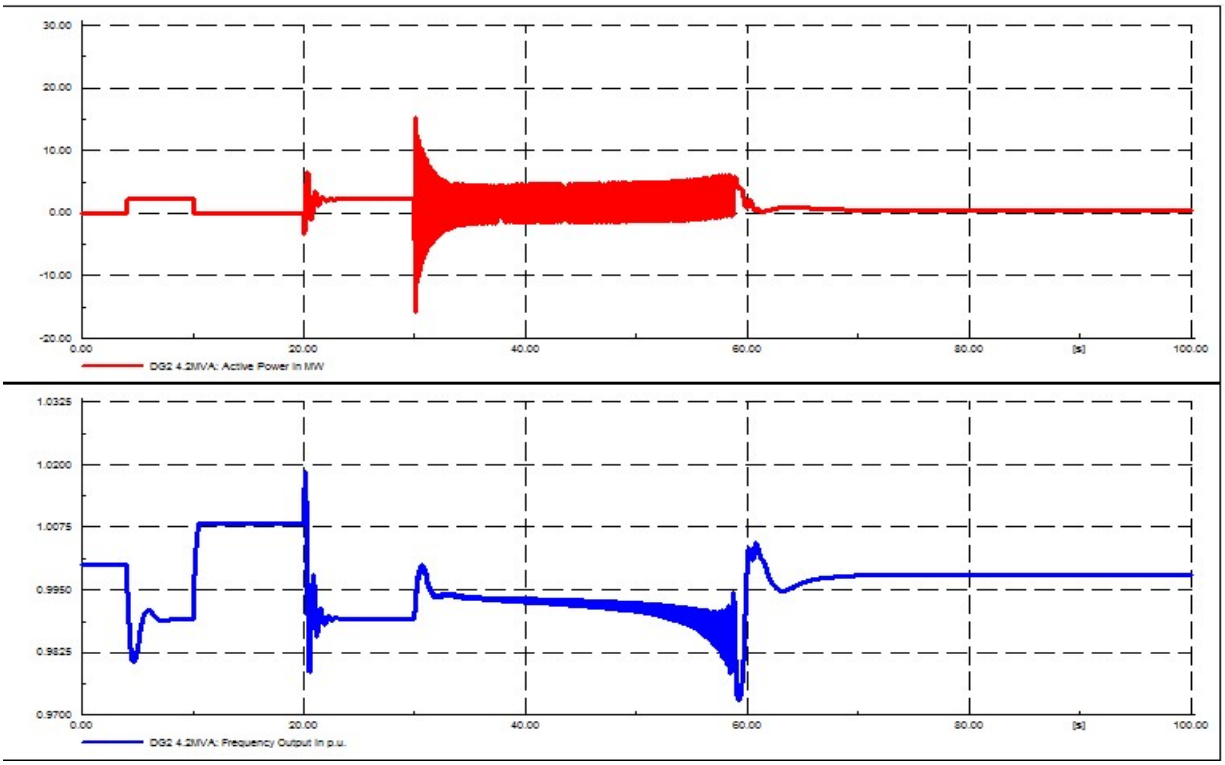

Figure 35: DG2 response to grid-restoration

Voltage regulation for DG2 is similar to DG1 as shown in Figure 36, as described above in 5.2.1.1.

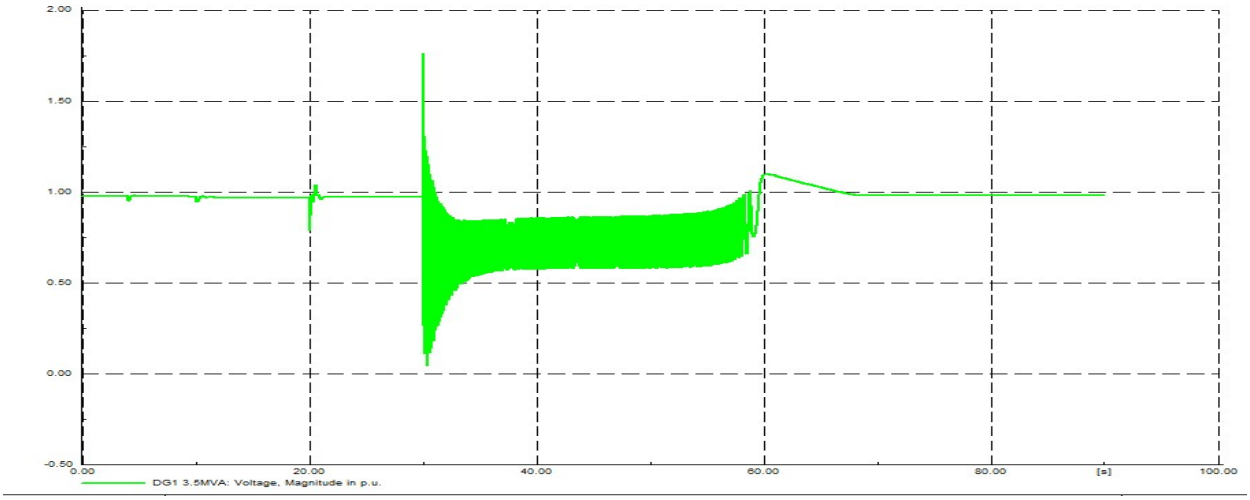

Figure 36: DG2 voltage response

5.2.2.3 DG3 response

As shown in Figure 37, DG3 has an active power response that shows an increase from 0MW to 1.5MW when the microgrid is disconnected from the main grid. It

then maintains this power output until DG2 is disconnected, where the output power is increased to 2.4MW, as expected to meet the load requirements. When DG2 is reconnected at t=10s, the output power from DG3 responds by oscillating, ranging from -0.4MW to 4.1MW over a period of 1.5s before achieving a steady-state output of 1.5MW again. The increase in common load event does not impact the output power, as per the other DGs. The next event that impacts DG3 output power is when the main grid is restored, Figure 38, which causes oscillations ranging from -12.5MW to 10.5MW over 30s to reach a steady-state output power of 0MW as expected. This is the same as before the grid disconnection. For the frequency response, DG3 has a similar response to the changes in DG1, where the frequency drops to 0.9807pu (49.0 Hz), recovers to 0.9889pu (49.4 Hz) before another drop, when DG2 is disconnected, to 0.9779pu (48.9 Hz). The DG frequency is then restored to 0.9830pu (49.2 Hz) until DG2 is reconnected at t=20s. The common load increase has minimal impact to the DG frequency. When DG2 is reconnected, DG3 frequency output oscillates with a drop to 0.9767pu (48.8 Hz) and peaks at 1.0024pu (50.0Hz) before achieving a steady-state frequency output of 0.9890pu (49.5 Hz) after 2.6s. The DG output frequency remains at this value until the main grid is reconnected, where it undergoes frequency oscillations ranging between 0.9726pu (48.6 Hz) and 1.0036pu (50.2 Hz) over a period of 30s, before achieving a steady-state frequency of 0.9980pu (49.9 Hz). Through the transitions the DG frequency remains within the limits defined in Appendix A, Table 3[11].

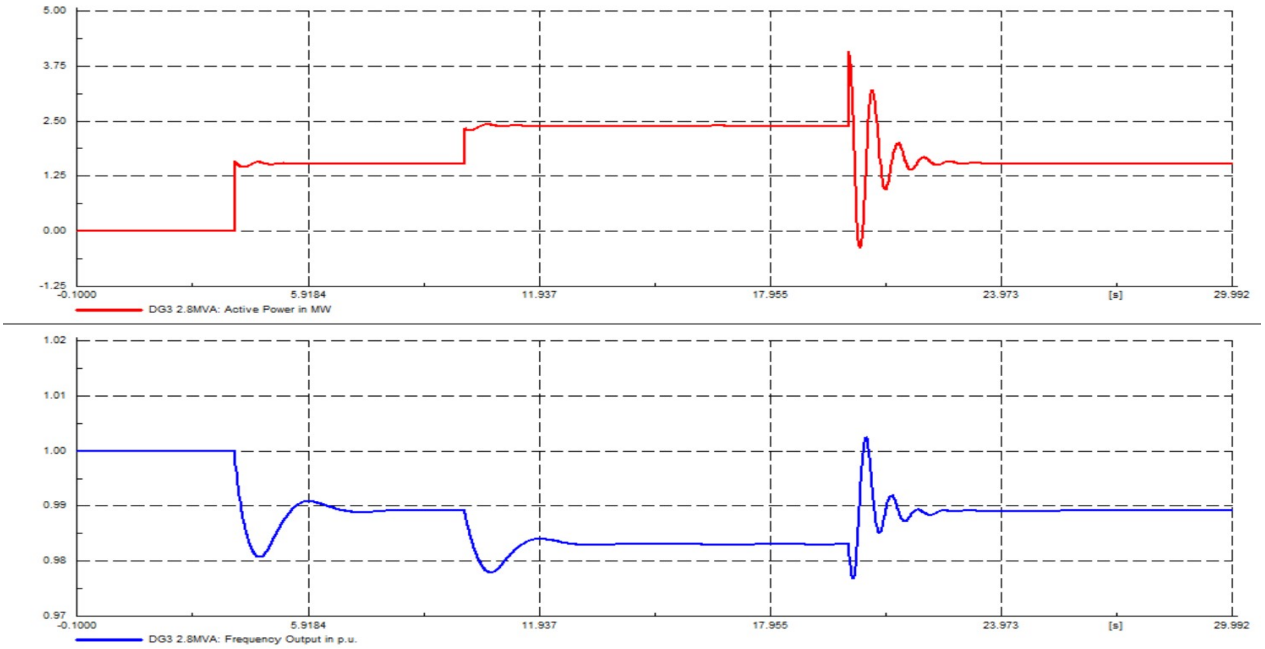

Figure 37: DG3 power-frequency response

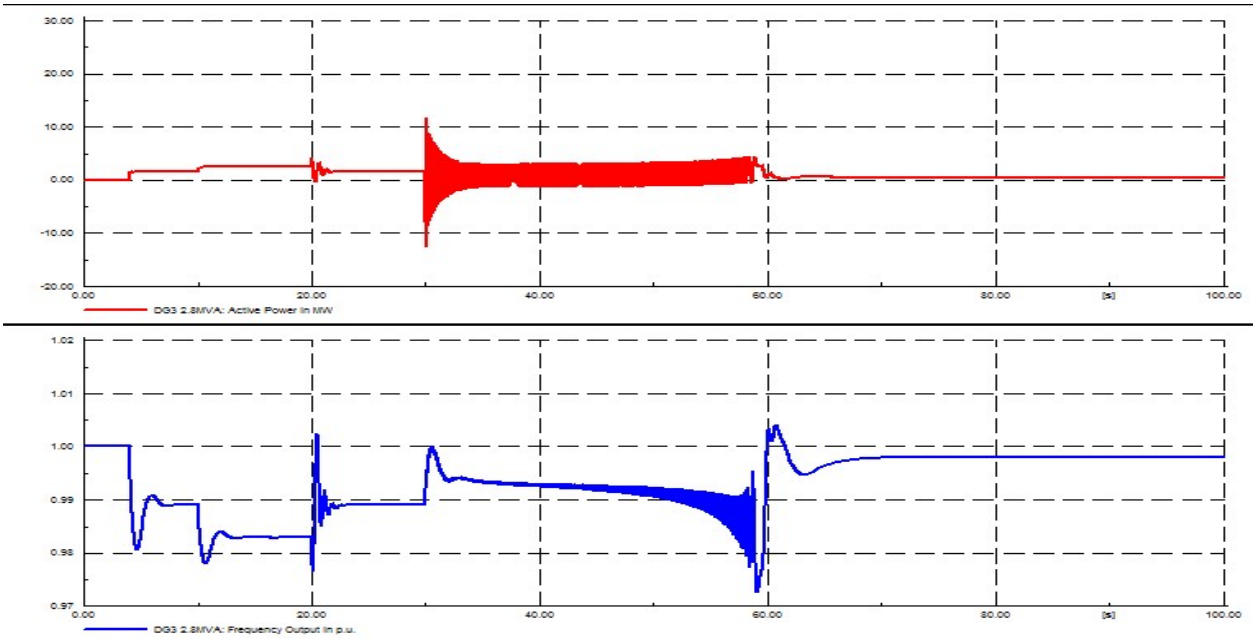

Figure 38: DG3 response to grid-restoration

Voltage regulation for DG3 is similar to DG1 as shown in Figure 39, as described above in 5.2.1.1.

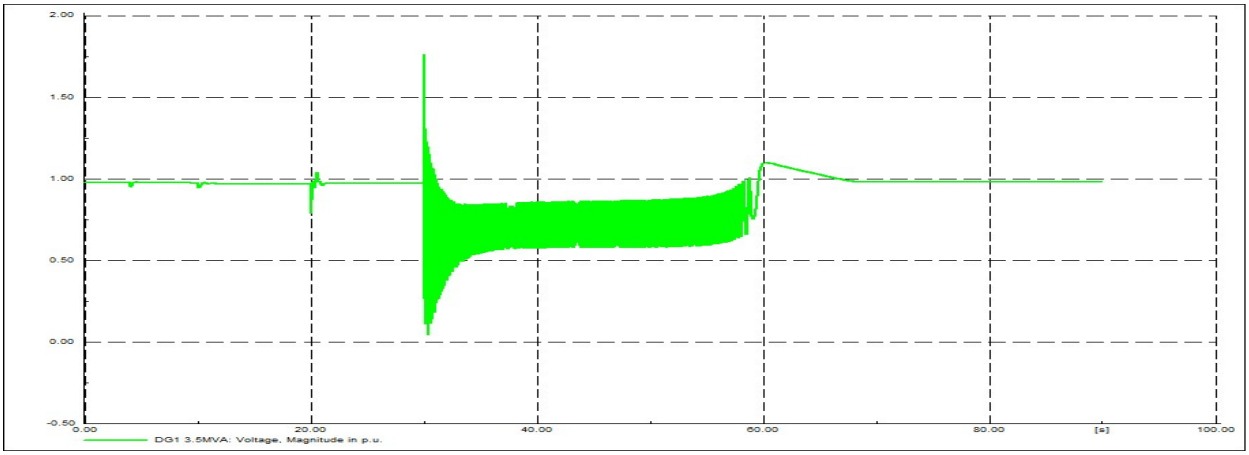

Figure 39: DG3 voltage response

Overall, from the analysis of the controller, it is clear that the three DG units' performance in relation to active power sharing and frequency control comply with the grid standard.

Chapter 6

6 Conclusion & Recommendation for Future Work

6.1 Conclusion

The investigation conducted during this thesis included methods of microgrid control, through the modes of operation when connected to the main electrical grid, including grid-connect, islanded and transitioning between the two. The issues and problems encountered with microgrid control were discussed and covered areas such as voltage and frequency regulation, islanding operation and the protection schemes used. Further, the hierarchy of control was summarised for the primary, secondary and tertiary control methods.

Common methods of control including the use of SMO and MMO for the voltage and frequency regulation were discussed and alternative methods such as the DPC method and the allocation of fixed and switching capacitors were also presented. Also investigated was the use of SG and VSI-based droop control based on voltage, frequency, angle and cooperative droop methods. This was beneficial in allowing the reader to have an understanding of the different methods of not only microgrid control, but specifically droop control for better voltage, frequency regulation and active power sharing between different generator microsources within the microgrid.

The use of DIgSILENT PowerFactory™ allowed for the simulation to be conducted using governor (primary) control and power-frequency (secondary) control scenarios on different network configurations including non-grid and grid-connected. This was supported by some development with the MatLab Simulink environment but was deliberately limited to ensure the simulations were maintained with the PowerFactory software simulation environment. This did cause some issues in relation to the import of control strategies which would require further investigation and was due to unfamiliarity with the simulation environment.

Overall this thesis report is based on research of the different control strategies and how they are implemented within a microgrid, with simulations conducted to support the areas of governor and power-frequency control for a synchronous generator. VSI-based droop control was investigated but not simulated and would be the next step if the investigation of this type of control. The P-f droop control and governor methods were assessed against the Western Power Technical Rules [1], though further investigation into a real-world microgrid would assist with the consolidation of the research. It was found that SG control with a governor, AVR and P-f controller maintained compliance within the limits, with the exception of grid-restoration events causing exceedance of the required limits set by the standard, but could be regarded as a contingency event therefore remaining compliant.

6.2 Recommended Further Work

The purpose of this thesis was to research microgrid control strategies, including droop control, using examples of the load and switch events that could occur during the operation and management of a microgrid. As the report does not cover the simulation and comparison of angle-frequency or virtual flux droop methods, there is benefit in extending the research to investigate these further

It is also suggested that the simulation of an actual microgrid be modelled, including wind-turbines, and photovoltaics arrays, using the PowerFactory simulation software package. The impact of the different control methods could be investigated to provide a good basis for future researchers to build upon. Additionally a small bench-top microgrid model with supporting documentation is also suggested for future investigation, as this would be a valuable tool in the education of future student and researchers.

Bibliography

[1] S. M. Ashabani and Y. A. I. Mohamed, "General Interface for Power Management of Micro-grids Using Nonlinear Cooperative Droop Control," *IEEE Transactions on Power Systems,* vol. 28, no. 03, pp. 2229-2941, 2013.

[2] N. L. Diaz, T. Dragicevic, J. C. Vasquez and J. Guerrero, "Intelligent Distributed Generation and Storage Units for DC Microgrids - A New Concept on Cooperative Control without Communications Beyond Droop Control," *IEEE Transactions,* vol. 5, no. 05, pp. 2476-2485, 2014.

[3] A. R. Salechinia, M. R. Haghifam and M. Shahabi, "Reactive Power Control in a Microgrid in both Grid-Connected and Islanding Modes of Operation," in *21st International Conference on Electricity Distribution*, Frankfurt, 2011.

[4] R. H. Lasseter, "Microgrids," *In Power Enginering Society Winter Meeting,* vol. 1, pp. 305-308, 2002.

[5] A. A. Salam, A. Mohamed and M. A. Hannan, "Technical Challenges on Microgrids," *ARPN Journal of Engineering and Applied Science,* vol. 3, no. 6, pp. 64-69, 2008.

[6] S. M. Ashabani and A.-r. I. Mohamed, "New Family of Microgrid Control and Management Strategies in Smart Distribution Grids - Analysis, Comparison and Testing," *IEEE Transactions on Power Systems,* vol. 29, no. 05, pp. 2257-2269, 2014.

[7] J. C. Vasquez, J. M. Guerrero, J. Miret, M. Castilla and L. G. de Vicuna, "Hierarchical Control of Intelligent Microgrids," *industrial Electronics Magazine,* vol. 4, no. 4, pp. 23-29, 2010.

[8] F. Aljawder, "Control of a Microgrid in Islanded Mode," Murdoch University, Perth WA, 2012.

[9] R. Majumder, A. Ghosh, G. Ledwich and F. Zare, "Operation and Control of Hybrid microgrid with Angle Droop Control," IEEE, 2010.

[10] P. Basak, U. Jadavpur, I. Kolkata, A. K. Saha, S. Chowdhury and S. P. Chowdhury, "Microgrid: Control techniques and modelling," in *Universities Power Engineering Conference (UPEC)*, Glasgow, 2009.

[11] Western Power, "Technical Rules," Western Power, Perth, 2011.

[12] T. L. Vandoorn, B. Meersman, K. J. D. M. Kooning and L. Vandevelde, "Transition from Islanded to Grid-Connected Mode of Microgrids with Voltage-Based Droop Control," *IEEE Transactions on Power Systems,* vol. 28, no. 03, pp. 2545-2553, 2013.

[13] M. Dewadasa, "Protection of distrinuted generation interfaced networks," Queensland University of Technology, Queensland, 2010.

[14] E. D. Spooner, "A New Australian Standard for Small Grid-Connected Renewable Generation Systems Connected via Inverters," ACRE, The University of NSW, Sydney, 2001.

[15] J. M. Guerrero, J. C. Vasquez, J. Matas, L. G. d. V. Vicuna and M. Castilla, "Heirarchical Control of Droop-Controlled AC and DC Microgrids - A General Approach Toward Standardization," *IEEE Transactions on Industrial Electronics,* vol. 58, no. 01, pp. 158-172, 2011.

[16] J. A. Lopes, C. L. Moreira and A. G. Madureira, "Defining Control Strategies for MicroGrids Islanded Operation," *IEEE Transactions,* vol. 21, no. 02, pp. 916-924, 2006.

[17] A. Bidram and A. Davoudi, "Hierarchical Structure of Microgrids Control System," *IEEE Transactions on Smart Grid,* vol. 3, no. 4, pp. 1963-1976, 2012.

[18] J. G. Norniella, J. M. Cano, G. Orcajo, C. H. Rojas, J. F. Pedrayes, M. F. Cabanas and M. G. Melero, "Multiple switching tables direct power control of active front-end rectifiers," *IET Power Electronics,* vol. 7, no. 06, pp. 1578-1589, 2014.

[19] R. Majumder, A. Ghosh, G. Ledwich and F. Zare, "Angle Droop versus Frequency in a Voltage Source Converter based Autonomous Microgrid," IEEE, 2009.

[20] DIgSILENT, PowerFactory Version 15 User Manual, Gomaringen, Germany: DIgSILENT, 2014.

[21] B. Idlbi, "Dynamic Simulation of a PV-Diesel-Battery Hybrid Plant for Off-Grid Electricity Supply," Cairo University, Cairo, 2012.

[22] S. J. Chapman, Electric Machinery Fundamentals, New York: McGraw-Hill, 2012.

[23] J. A. P. Lopes and F. O. R. Moreira, "Control Strategies for Microgrids Black Start and Islanded Operation," *International Journal of Distributed Energy Resources,* vol. 1, no. 3, pp. 241-261, 2005.

[24] K. D. Brabandere, B. Bolsens, J. V. d. Keybus, A. Woyte, J. Driesen and R. Belmans, "A Voltage and Frequency Droop Control Method for Parallel Inverters," *IEEE Transactions on Power Electronics,* vol. 22, no. 04, pp. 1107-1115, 2007.

[25] M. C. Chandorkar, D. M. Divan and R. Adapa, "Control of parallel connected inverters in standalone AC systems," *IEEE Transactions on Industry Applications,* vol. 29, no. 1, pp. 136-143, 1993.

[26] J. Hu, J. Zhu, D. G. Dorrell and J. M. Guerrero, "Virtual Flux Droop Method - A New Control Strategy of Inverters in Microgrids," *IEEE Transactions on Power Electronics,* vol. 29, no. 9, pp. 4704-4711, 2014.

[27] "Version 14.1 PowerFactory User Library," DIgSILENT, Gomaringen, Germany, 2013.

[28] B. Sedaghat, A. Jalilvand and R. Noroozian, "Design of a multilevel control strategy for integration of stand-alone wind/diesel system," *International Journal of Electrical Power & Energy Systems,* vol. 35, no. 1, pp. 123-137, 2012.

[29] D. G. Holmes, R. Kabiri and B. P. McGrath, "DigSILENT Modelling of Power Electronic Converters for Distributed Generation Networks," RMIT University, Melbourne.

[30] R. Kabiri, D. G. Homles and B. P. McGrath, "Inverter control modelling for distributed generation feeding into a utility network," in *Power Engineering Conference (AUPEC)*, Hobart, TAS, 2013.

Appendix A: Voltage & Frequency Operating Standards – SWIN

Voltage Regulation [11]

The steady-state voltage for a system connected to the SWIN, operating below 6kV must be within:

a) +/- 6% of the nominal voltage during normal operating state;

b) +/- 8% of the nominal voltage during maintenance conditions; and

c) +/- 10% of nominal voltage during emergency conditions.

For switching events the transmission voltages must be between 90% and 110% of nominal voltage, and the transmission systems must attain the previous setpoint in the final steady-state.

Infrequent switching events such as tripping of generators, loads, lines and other components have a limit of + 6% and -10%.

Frequency regulation [11]

Table 3: Frequency operating standards for the South West Interconnected System

Condition	Frequency Band	Target Recovery Time
Normal Range:		
South West	49.8 to 50.2 Hz for 99% of the time	
Island	49.5 to 50.5 Hz	
Single *contingency event*	48.75 to 51 Hz	Normal Range: within 15 minutes. For over-*frequency* events: below 50.5 Hz within 2 minutes.
Multiple *contingency event*	47.0 to 52.0 Hz	Normal Range within 15 minutes For under-*frequency* events: (a) Above 47.5 Hz within 10 seconds (b) Above 48.0 Hz within 5 minutes (c) Above 48.5 Hz within 15 minutes For over-*frequency* events:

		(d) Below 51.5 Hz within 1 minute (e) Below 51.0 Hz within 2 minutes (f) Below 50.5 Hz within 5 minutes

Appendix B: PowerFactory Model Parameters

Governor Parameters

Table 4: DG Governor Parameters

Model Definition:	DEGOV1		
Parameter	**Units**	**Description**	**Value**
K	[pu/pu]	Actuator Gain	9
T4	[s]	Actuator Derivative Time Constant	0.35
T5	[s]	Actuator First Time Constant	0.002
T6	[s]	Actuator Second Time Constant	0.015
TD	[s]	Combustion Delay	0.024
Droop	[pu]	Active Power / Frequency Deviation	0.02
TE	[s]	Time Constant Power Feedback	0.5
T1	[s]	Electric Control Box First Time Constant	0.018
T2	[s]	Electric Control Box Second Time Constant	0.001
T3	[s]	Electric Control Box Derivative Time Constant	0.38
Droop Control	-	(0=Throttle Feedback, 1=Elec. Power Feedback)	1
PN	[MW]	Prime Mover Rated Power (=0->PN=Pgnn)	0.816
Tmin	[pu]	Minimum Throttle Torque	0
Tmax	[pu]	Maximum Throttle Torque	1.2

Automatic Voltage Regulator (AVR) Parameters

Table 5: DG AVR Parameters

Model Definition:	avr_IEEET1		
Parameter	**Units**	**Description**	**Value**
Tr	[s]	Measurement Delay	0.02
Ka	[pu]	Controller Gain	150
Ta	[s]	Controller Time Constant	1
Ke	[pu]	Exciter Constant	0
Te	[s]	Exciter Time Constant	0.001
Kf	[pu]	Stabilisation Path Gain	0.1
Tf	[s]	Stabilisation Path Time Constant	6
E1	[pu]	Saturation Factor 1	1
Se1	[pu]	Saturation Factor 2	10
E2	[pu]	Saturation Factor 3	2
Se2	[pu]	Saturation Factor 4	0
Vrmin	[pu]	Controller Output Minimum	0.816
Vrmax	[pu]	Controller Output Maximum	0

Appendix C: Implemented PowerFactory Models

2DG Model – Islanded

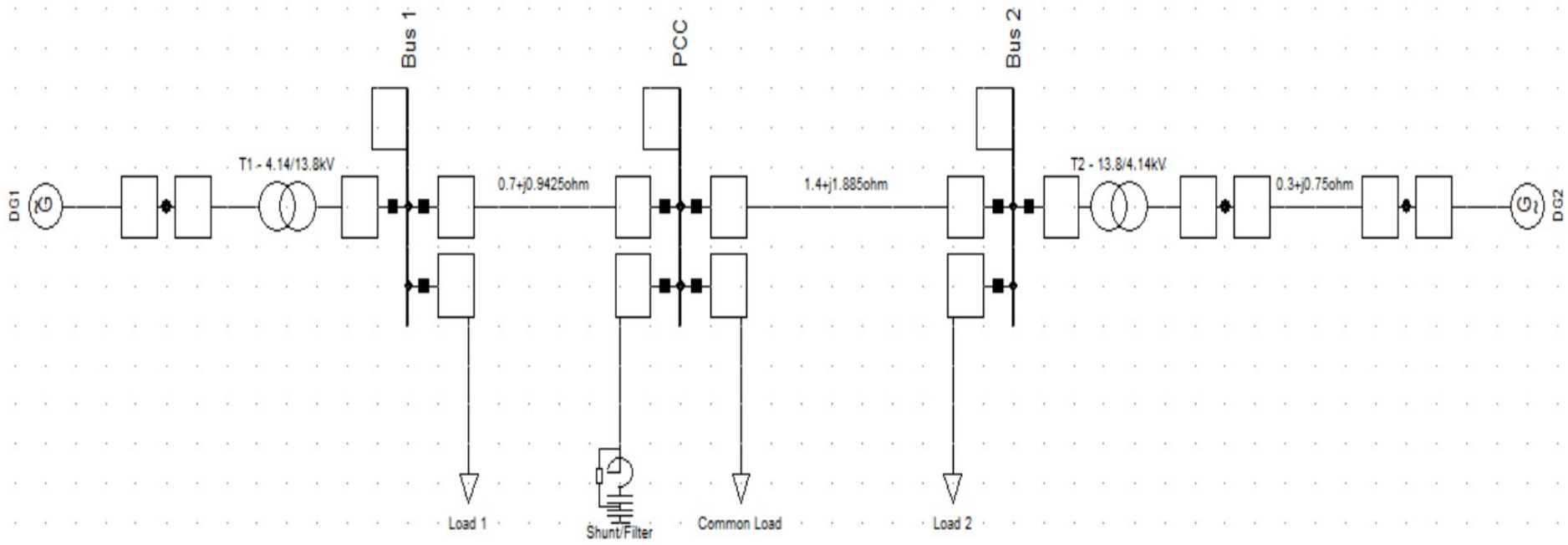

Figure 40: 2DG PowerFactory Model

3DG Model – Grid Connected

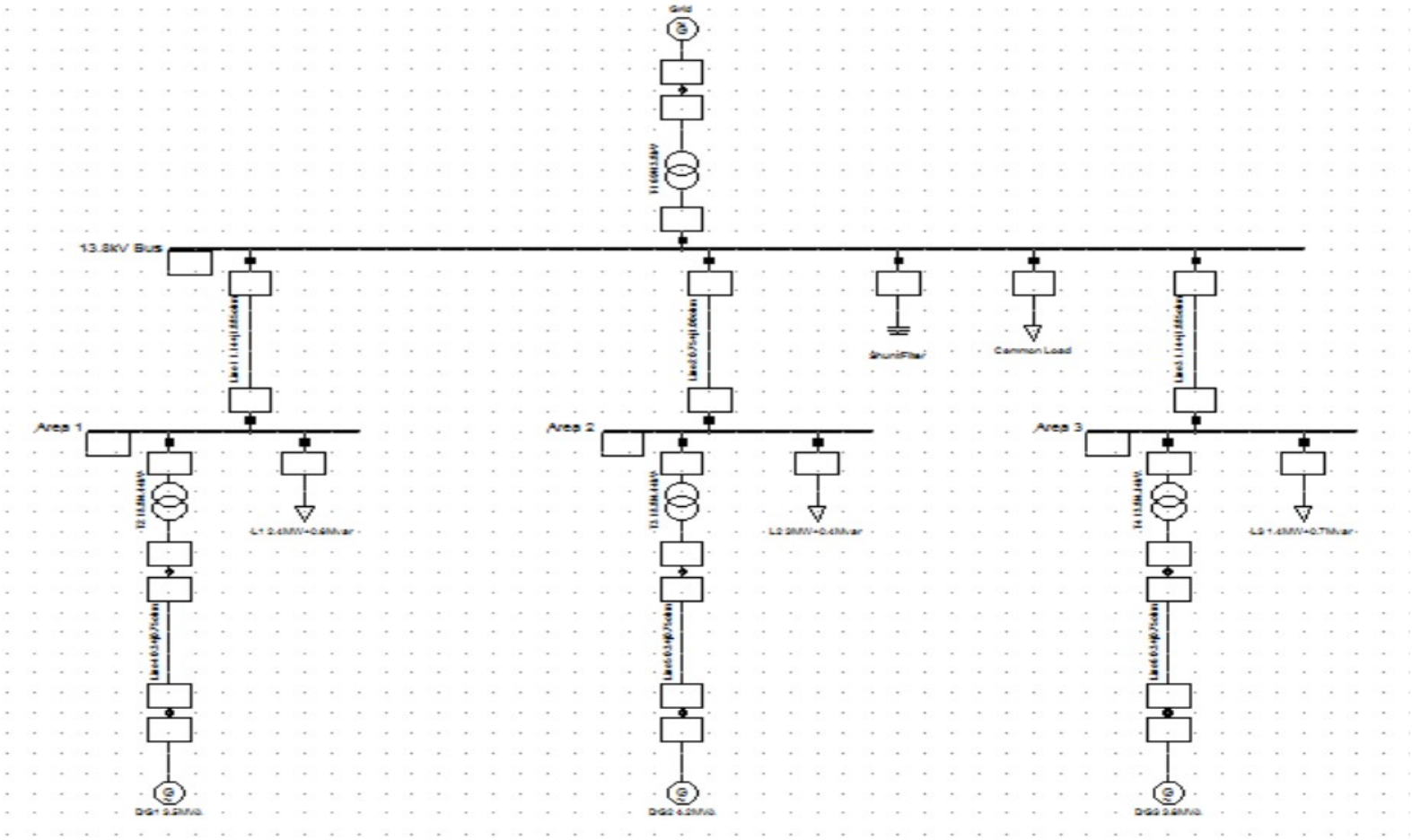

Figure 41: 3DG PowerFactory Model